SKB

TECHNICAL REPORT 89-09

An evaluation of tracer tests performed at Studsvik

Luis Moreno[1], Ivars Neretnieks[1], Ove Landström[2]

[1] The Royal Institute of Technology, Department of Chemical Engineering, Stockholm

[2] Studsvik Nuclear, Nyköping

March 1989

SVENSK KÄRNBRÄNSLEHANTERING AB
SWEDISH NUCLEAR FUEL AND WASTE MANAGEMENT CO

BOX 5864 S-102 48 STOCKHOLM
TEL 08-665 28 00 TELEX 13108-SKB

AN EVALUATION OF TRACER TESTS PERFORMED AT STUDSVIK

Luis Moreno[1], Ivars Neretnieks[1], Ove Landström[2]

1 The Royal Institute of Technology, Department of Chemical Engineering, Stockholm
2 Studsvik Nuclear, Nyköping

March 1989

AN EVALUATION OF TRACER TESTS PERFORMED AT STUDSVIK

Luis Moreno
Ivars Neretnieks
Ove Landström

March, 1989

KAT 89/01

ABSTRACT

In situ tracer tests performed with nonsorbing tracers, as well as with sorbing tracers, in crystalline rock at the Studsvik site in Sweden have been analysed. Three different models were used: Advection-Dispersion model, Advection-Dispersion-matrix Diffusion model, and Advection-Channeling-matrix Diffusion model. Tests with a nonsorbing tracer were used to obtain information on hydraulic properties and tests with a sorbing tracer were used to determine the sorption properties of the fractured rock.

TABLE OF CONTENTS

SUMMARY

In situ tracer tests performed with nonsorbing tracers, as well as with sorbing tracers, in crystalline rock at the Studsvik site in Sweden were analysed using three different models. The Advection-Dispersion model considers only sorption onto the surface of the fractures. The Advection-Dispersion-matrix Diffusion model includes diffusion into the rock matrix and sorption within it. The Advection-Channeling-matrix Diffusion model takes into account the tracer dispersion by channeling. Tests with a nonsorbing tracer, tritiated water, were used to obtain information on hydraulic properties and tests with the sorbing tracer strontium were used to determine the sorption properties of the fractured rock. The nonsorbing tracer tests showed a high dispersion which could have been caused by several mechanisms. Some of the possible causes probably were zones with near stagnant water or the presence of channels with different water residence times. The models used in this report do not quantitatively take into account these mechanisms because of the lack of information. One of the main difficulties in analysing these tests is due to channeling effects. The injection of the tracers did not seem to have taken place in the main flow path(s). Also the observed residence time of the tracers did not seem to bear any relation to the main flowrate in the system. This made it impossible to assess the fracture characteristics (aperture) and to make meaningful predictions of the transport of sorbing species.

The low recovery of the sorbing tracer observed in these tests may have been caused by several factors. However, with the existing experimental data it still was not possible to determine which mechanism caused the low recovery of strontium.

1 INTRODUCTION

In Sweden, crystalline rock has been selected as the most suitable bedrock in which to build a repository for radioactive waste. If a canister is broken, the radionuclides will be carried by the water flowing through the fractures in the bedrock. The radionuclides may interact with the rock by means of diffusion into the rock matrix and by sorption onto the surface of the fractures and microfractures.

The prediction of the behavior of radionuclides escaping from a repository requires the use of models which adequately describe the transport of the radionuclides by the groundwater flow. Experimental determinations of the sorption capacity of the rock and the effective diffusion of the species into the rock matrix have been made in the laboratory (Skagius et al., 1982; Skagius, 1986; Skagius and Neretnieks, 1986a, 1986b, 1988; Andersson et al., 1983).

Tracer tests in situ may be used to test these models and the data obtained in the laboratory. In Sweden various field experiments have been performed in Finnsjön (Gustafsson and Klockars, 1981, 1984), Studsvik (Landström et al., 1978, 1983), and Stripa (Abelin et al., 1985; Andersson and Klockars, 1985).

The tracer test carried out in the Studsvik area by Landström et al. (1983) have been used to test three different models for the tracer transport in crystalline rock. Tests with nonsorbing tracers give information on the hydraulic properties of the fractures and the water flow. Tests with sorbing tracers are used to study the sorption capacity of the rock.

2 EXPERIMENTS

The tracer tests were carried out at Studsvik by Landström et al. (1983). A cutaway view of the in situ test site is shown in Figure 2-1. Two flow pathways were studied: B1N-B6N and B5N-B6N. Tracers were injected at the holes B1N and B5N. Water was continuously pumped up in the hole B6N. Tracers were injected between two packers spaced at a distance of 1.2 - 1.3 m.

Tracers were injected for 50 min. The injection flowrate was 0.01 lmin. Water was injected with the same flowrate before and after the injection of the tracer. The pumping flowrate was 1.2 l/min. The water flow in the pathways was estimated to be 0.096 l/min for B1N-B6N and 1.02 l/min for B5N-B6N. The difference in pressure heads was 3.0 and 2.5 m for the flow paths B1N-B6N and B5N-B6N, respectively. The distances between injection and detection holes were 11.8 and 14.6 m for the tracer tests B1N-B6N and B5N-B6N, respectively.

H-3 and I-131 were used as nonsorbing tracers. Strontium was used as the sorbing tracer. The I-131 curve in both experiments was almost identical with that of H-3. In the hole B5N, cesium was also injected but it was not detected in B6N.

The breakthrough curves are shown in Figures 2-2 - 2-5. In the run B1N-B6N, 93 % of the tritiated water was recovered during the observation time. The recovery of the strontium was only about 6 % during the same time. The values for the run B5N-B6N were 96 % and 18 % for tritiated water and strontium, respectively.

The rock type at the test site is a gneiss of sedimentary origin. Holes B1N, B5N, and B6N were hammer-drilled and 115 mm in diameter. Filling material from a core drilled at the test site was studied. Most of the fractures observed in the core were coated and open. Many of these fractures, however, probably were opened during the drilling operation (Landström et al., 1983). Most of the coated fractures were thin, usually less than 1 mm, and mainly coated with chlorite and calcite.

The experimental data are shown in Appendix A. The location of the packers and the length of the flow paths are shown in Table B-1 in Appendix B. Table B-2 shows the data for the tracers used in these runs.

3 MECHANISMS

When tracers flow through a fracture or fracture system they will be dispersed. If the effect of the rock matrix is not considered, the following mechanisms are known to affect the transport:

- Molecular diffusion in the liquid in the fracture
- Mechanical dispersion in the liquid in the fracture due to velocity variations in the fluid
- Channeling
- Sorption onto the surface of the fracture.

Molecular diffusion results from the differences in tracer concentration within the liquid phase. Because molecular diffusion effects depend on time, their effects on the overall dispersion will be more significant at low velocities. The molecular diffusion in the liquid in the fractures in the direction of the flow is negligible compared to the mechanical dispersion in in situ experiments.

The rock matrix contains a connected system of microfractures. Through these microfractures the tracers can diffuse into the rock matrix by molecular diffusion even when flow does not take place in the matrix due to its low permeability. The tracers that penetrate into the rock matrix can be sorbed onto the surfaces of the microfractures. If the matrix is porous the following mechanisms may affect the transport in addition to those above:

- Molecular diffusion into the rock matrix
- Sorption onto the surface of the microfractures within the rock matrix.

Several more or less distinct flow paths may exist between the injection and pumping holes.

The flow takes place in different channels with different velocities. In this case, tracers are dispersed by what we call channeling dispersion.

The interaction of the tracer with the surface of the fractures or microfractures is accounted for by assuming a reversible and instantaneous reaction.

If a linear equilibrium reaction is assumed between the tracer concentration in the fluid and the tracer concentration sorbed on the surface of the solid, then the equilibrium relationship can be written

$$C_s = K_a\, C_f \tag{3.1}$$

It is possible to define the surface retardation factor, R_a, as

$$R_a = 1 + \frac{2}{\delta}\, K_a \tag{3.2}$$

For a bulk reaction where the solid is penetrated throughout and the tracer is sorbed onto the surface of the microfractures, a volume sorption coefficient is defined. The volume sorption coefficient considers the equilibrium between the tracer concentration in the pore fluid and the tracer concentration within the solid

$$C_m = K_d'\, C_p \tag{3.3}$$

In this case the mass sorption coefficient, K_d', is based on the mass of the solid proper.

The definition of the mass equilibrium coefficient is sometimes based on the mass of the microfracture solid and includes the nuclide that is in the water in the microfractures as well as that in the solid

$$K_d\, \rho_p = \varepsilon_p + (1 - \varepsilon_p)\, K_d'\, \rho_p \tag{3.4}$$

For a nonsorbing substance ($K_d'=0$), the porous rock matrix still has a mass equilibrium constant equal to ε_p/ρ_p due to the uptake of tracers in the pores.

The following models will be used to analyse the experimental breakthrough curves:

- The Advection-Dispersion model - AD
- The Advection-Dispersion-matrix Diffusion model - ADD
- The Advection-Channeling-matrix Diffusion model - ACD.

3.1 THE ADVECTION-DISPERSION MODEL - AD

This model considers that the transport of the tracers from the injection point to the detection point takes place through a parallel walled fracture. The interaction between the tracer and the solid material is limited only to the walls of the fractures (surface sorption mechanism). The following mechanisms are included in the model:

- Advective transport along the fracture
- Longitudinal hydrodynamic dispersion in the fracture
- Sorption onto the surface of the fracture.

The governing equation, including the surface sorption mechanism, for the tracer concentration in a fracture may be written

$$\frac{\partial C_f}{\partial t} + \frac{2}{\delta}\frac{\partial C_s}{\partial t} + U_f \frac{\partial C_f}{\partial x} - D_L \frac{\partial^2 C_f}{\partial x^2} = 0 \qquad (3.5)$$

Introducing the surface retardation factor defined in equation (3.2) into equation (3.5) results in

$$\frac{\partial C_f}{\partial t} + \frac{U_f}{R_a}\frac{\partial C_f}{\partial x} - \frac{D_L}{R_a}\frac{\partial^2 C_f}{\partial x^2} = 0 \qquad (3.6)$$

For these tests the initial and boundary conditions are

$$C_f(x,0) = 0$$
$$C_f(0,t) = m\,\delta(t)/Q \qquad (3.7)$$
$$C_f(\infty,t) = 0$$

The solution for the differential equation with its corresponding initial and boundary conditions is given by Lenda and Zuber (1970)

$$C_f = \frac{m}{V}\left(\frac{Pe}{4\pi\, t_R^3}\right)^{1/2} \exp\left(-\frac{Pe}{4\, t_R}\,(1 - t_R)^2\right) \qquad (3.8)$$

where

$$t_R = t/t_o$$
$$Pe = U_f\, x/D_L$$
$$t_o = R_a\, t_w$$

3.2 THE ADVECTION-DISPERSION-MATRIX DIFFUSION MODEL - ADD

In the previous model only the interaction of the tracer with the surface of the walls of the fracture was included. The ADD model includes the interaction of the tracer with the interior of the rock matrix as well.

It is assumed that the advective transport of the tracers takes place through a single fracture. In addition the tracers penetrate into the rock matrix by molecular diffusion and they may be sorbed onto the fracture surface and within the rock matrix.

The model considers the transport of contaminants in a fluid which flows through a thin fracture in a water-saturated porous rock. The groundwater velocity in the fracture is assumed constant. The following processes are considered:

- Advective transport along the fracture
- Longitudinal hydrodynamic dispersion in the fracture
- Sorption onto the surface of the fracture
- Molecular diffusion from the fracture into the rock matrix
- Sorption onto the surface of the microfractures in the rock matrix.

The equation for the concentration in the fracture must include the surface sorption mechanism as well as the flux perpendicular to the plane of the fracture due to the diffusion into the rock matrix. Assuming a linear sorption isotherm for the surface sorption and using the surface retardation factor R_a, the differential equation for the fracture becomes

$$\frac{\partial C_f}{\partial t} - \frac{D_L}{R_a}\frac{\partial^2 C_f}{\partial x^2} + \frac{U_f}{R_a}\frac{\partial C_f}{\partial x} - \frac{2}{\delta}\frac{D_e}{R_a}\frac{\partial C_p}{\partial z}\Bigg|_{z=0} = 0 \qquad (3.9)$$

$$0 \le x \le \infty$$

For sorption within the porous rock matrix, a linear equilibrium isotherm is assumed, the differential equation for the (infinite) rock matrix can be written

$$\frac{\partial C_p}{\partial t} - \frac{D_e}{K_d \rho_p}\frac{\partial^2 C_p}{\partial z^2} = 0 \qquad 0 \le z \le \infty \qquad (3.10)$$

The injection in these experiments was designed to be a square pulse during a short time interval. The injection time is very short compared with the water residence time. So the injection may, in practice, be considered as a pulse injection. The concentration in the fracture for a pulse injection is (Maloszewski and Zuber, 1984)

$$\frac{C(t)}{C_o} = \frac{2}{\pi} \exp\left(\frac{Pe}{2}\right) \int_{\lambda}^{\infty} \frac{\frac{Pe\, t_o}{8\, A\, \xi^2}}{\left(t - \frac{Pe\, t_o}{4\, \xi^2}\right)^{3/2}} \cdot$$

$$\exp\left[- \xi^2 - \frac{Pe^2}{16\, \xi^2} - \frac{\frac{Pe^2\, t_o^2}{64\, \xi^4\, A^2}}{\left(t - \frac{Pe\, t_o}{4\, \xi^2}\right)} \right] d\xi \qquad (3.11)$$

where

$$\lambda = \left(\frac{Pe\, t_o}{4\, t}\right)^{1/2}$$

$$Pe = \frac{U_f\, x}{D_L}$$

$$t_o = R_a \frac{x}{U_f} = R_a\, t_w$$

$$A = \frac{\delta\, R_a}{2\, (K_d\, \rho_p\, D_e)^{1/2}}$$

The integral in equation (3.11) is evaluated numerically by Gaussian quadrature. In our applications, for a sorbing tracer, the integrand is a well-behaved function. For short times and for nonsorbing substances, which give high values for the A-parameter, the function may be ill-behaved and the integration takes more effort.

For nonsorbing tracer tests, when the injection is not very short, it is more convenient to consider the injection as a square pulse with duration Δt. The concentration at the outlet is obtained using the solution for a step injection at the inlet. For a square pulse the solution for a step injection delayed in time by Δt is subtracted from the same function. The solution for a step function has been obtained by Tang et al. (1981).

3.3 THE ADVECTION-CHANNELING-MATRIX DIFFUSION MODEL - ACD

In the ACD model the dispersion that occurs in the direction of the flow is accounted for by means of channeling dispersion. The model is based on the following concept. The flow between injection and observation point occurs through a multitude of independent channels. The velocity differences in the channels will carry a tracer different distances over a given time. When the fluid from all the channels is mixed at the observation point (withdrawal by pumping), the different arrival times in the various channels will cause a pulse to spread. The observer will see a dispersed pulse.

The transport of the tracers takes place through a fracture in which parallel channels with different apertures exist. This is shown in Figure 3-1. It is assumed that the channel apertures have a lognormal distribution and the interconnection between the different channels is negligible. The hydrodynamic dispersion in each individual channel is also assumed to be negligible compared to the effects of channeling. The model includes the following mechanisms:

- advective transport along the fracture
- channeling dispersion
- sorption onto the surface of the channels
- diffusion into the rock matrix
- sorption within the rock matrix.

For a tracer flowing through a fracture with negligible longitudinal dispersion, the equation for the concentration in the fracture is

$$\frac{\partial C_f}{\partial t} + \frac{U_f}{R_a}\frac{\partial C_f}{\partial x} - \frac{2}{\delta}\frac{D_e}{R_a}\frac{\partial C_p}{\partial z}\Bigg|_{z=0} = 0 \qquad (3.12)$$

The equation for the diffusion into the rock matrix is given as before by equation (3.10). The solution for equations (3.10) and (3.12) is found in the literature (Carslaw and Jaeger, 1959)

$$\frac{C_f}{C_o} = \text{erfc}\left(\frac{B\ t_w}{\delta\ (t - t_o)^{1/2}}\right) \qquad (3.13a)$$

Using the parameters in the ADD model, equation (3.13a) becomes

$$\frac{C_f}{C_o} = \text{erfc}\left(\frac{t_o}{2\,A\ (t - t_o)^{1/2}}\right) \qquad (3.13b)$$

where

$$t_o = R_a\ t_w = \left[1 + \frac{2}{\delta} K_a\right] t_w$$

$$B = (D_e\ K_d\ \rho_p)^{1/2}$$

If in each pathway separate channels exist with different apertures, δ, then the fluid will have different velocities in the different channels when flowing through the fracture. In this case R_a will be different for the different channels. The constant entity is K_a, the surface equilibrium coefficient. The entity A will in this case vary with δ and it is more appropriate to use the entity B which is constant. If the breakthrough curve for each channel in the actual pathway is given as

$C_f(\delta,t)$, then the concentration of the mixed effluent from all the channels in the pathway is (Neretnieks et al., 1982)

$$\frac{C(t)}{C_o} = \frac{\int_0^\infty f(\delta)\, Q(\delta)\, C_f(\delta,t)\, d\delta}{\int_0^\infty f(\delta)\, Q(\delta)\, d\delta} \qquad (3.14)$$

In a parallel-walled channel of aperture δ, the flowrate for laminar flow is proportional to the fracture aperture cubed. Snow (1970), studying the fracture frequencies for consolidated rock, found that the fracture apertures have a lognormal distribution. The density function has the form

$$f(\delta) = \frac{1}{\sigma\sqrt{2\pi}}\,\frac{1}{\delta}\,\exp\left(-\frac{[\ln(\delta/\mu)]^2}{2\sigma^2}\right) \qquad (3.15)$$

4 GOVERNING EQUATIONS FOR THE FLOWRATE

In tracer tests with radial flow through a fracture, the hydraulic conductivity of the fracture is determined by integration of Darcy's equation

$$K_{pf} = \frac{1}{2} \frac{\ln \left(\frac{r_2}{r_1}\right) \left(r_2^2 - r_1^2\right)}{\left(h_2 - h_1\right) t_w} \tag{4.1}$$

The radial velocity in the fracture at radius r may be calculated from

$$U_r = \frac{1}{r} \frac{\left(h_2 - h_1\right)}{\ln \left(r_2 / r_1\right)} K_{pf} \tag{4.2}$$

If the water residence time is known, the water velocity may be evaluated directly by means of

$$U_r = \frac{1}{2r} \frac{\left(r_2^2 - r_1^2\right)}{t_w} \tag{4.3}$$

4.1 FRACTURE APERTURES

Observations indicate that fractures are closed in some parts and open in other parts. The opening thus may vary considerably over the plane of the fracture. Water possibly flows through a network of channels with unknown extension. So, any definition of an average fracture aperture implies some assumptions on its properties.

For a perfectly planar fracture with smooth walls and a constant opening, only one value should be needed to define the fracture aperture. Properties such as water residence time and pressure drop would be calculated using this fracture aperture. In a

fracture with varying openings and possibly with filling material this would not be possible.

One of the fracture properties of interest is the volume of the fracture. This could be determined from measuring the flowrate through the fracture and the water residence time. The fracture aperture thus calculated is called the mass balance fracture aperture, δ_f. For radial flow this may be expressed as

$$\delta_f = \frac{Q\, t_w}{\pi\,(r_2^2 - r_1^2)} \tag{4.4}$$

where Q is the flowrate through the fracture. When δ_f is calculated no assumptions are made on the geometry of the fracture and it is an averaged quantity.

Another fracture property of interest is the equivalent fracture aperture which would give a certain water velocity or residence time for a given pressure drop. This fracture aperture is called the frictional loss fracture aperture, δ_1. This is the aperture of a channel with parallel walls which would give the same resistance to the flow as the actual fracture. This aperture is expressed as

$$\delta_1 = \sqrt{K_{pf}\,\frac{12\,\upsilon}{g}} \tag{4.5}$$

A third interesting property is the equivalent fracture aperture which would permit a certain flowrate at a given pressure drop. This fracture aperture is called the cubic law fracture aperture, δ_c. It may be written as

$$\delta_c = 3\sqrt{\frac{6\,\upsilon\,Q}{g\,(h_2 - h_1)}\,\ln\frac{r_2}{r_1}} \tag{4.6}$$

5 RESULTS OF THE FITTING PROCESS USING THE ADVECTION-DISPERSION MODEL

The results of the tracer test B1N-B6N with tritiated water and strontium will be presented in this and the following sections. The results for the test B5N-B6N will be presented in Chapter 8 for the different models.

The experimental data are fitted using the Advection-Dispersion model assuming one and two pathways. For one pathway, the relative tracer concentration, $C(t)/C_O$, at the outlet of each fracture is a function of two parameters: Pe and t_O. If it is assumed that the tracer transport occurs through n pathways, the total concentration for a nonsorbing tracer is calculated by

$$C_f(t) = \sum_{i=1}^{n} pf_i \; C(Pe_i, t_{w\,i}, t) \qquad (5.1)$$

The factor pf takes into account the dilution effect and the tracer distribution between the fractures, and t_w is the water residence time.

The hydraulic properties determined from the nonsorbing tracer test are used to model the strontium test. For the sorbing tracer tests the surface retardation factor is determined in the fitting process. Due to the low recovery of strontium a loss factor was also included in the fitting process. The cause of the loss is not known at present and several possible causes are discussed.

For the sorbing tracer strontium the concentration in the detection hole is expressed as

$$C_f(t) = (1 - LF) \sum_{i=1}^{n} pf_i \; C(Pe_i, t_{wi}, R_i, t) \qquad (5.2)$$

where LF is the loss factor and R_i is the surface retardation factor in each pathway. Pe_i, t_{wi}, and pf_i are determined from the test with the nonsorbing substances.

If the fracture aperture δ can be determined, e.g., by a relationship between water residence time t_w and water flowrate in the fracture, the surface retardation factor may be written as equation (3.2). In this case the fit is reduced to two parameters: the loss factor and the surface sorption coefficient.

The agreement between the fitted breakthrough curves and the experimental data is studied by means of the standard deviation of the fitting process. The values of the fitted parameters including the 95 % confidence interval are given.

The fraction of the injected tracer which is recovered during the observation time and the theoretical recovery are also calculated. The theoretical recovery is the mass of tracer which would be recovered in an experiment with an infinite observation time.

5.1 RESULTS FOR THE NONSORBING TRACER TRITIATED WATER

The experimental recovery for the nonsorbing tracer tritiated water in the run B1N-B6 was 93 % during the observation time.

One and two pathways were used to fit the experimental data. The results are shown in Table 5-1 and Figures 5-1 and 5-2. When one pathway is used the fit is poor. The tracer recovery calculated from the fitted curve is only 48 % of the injected tracer. The model with two pathways shows a better agreement with the experimental data. This model may be improved by using three pathways, but in this case the parameters obtained in the fitting process would have a very low physical meaning.

Calculations were also made for a two pathway model assuming that the dispersivity is equal in both pathways. Assuming that the dispersion is proportional to the water velocity, the Peclet number is

$$Pe = \frac{U\ x}{D} = \frac{x}{\alpha} \qquad (5.3)$$

where α is the dispersivity. If the dispersivity is regarded as a property of the fractures, then the fractures with equal properties will give the same Peclet number. The fitting process was poor in this case considering the number of parameters fitted. The fracture properties which determine the hydrodynamic dispersion are different in the different fractures.

The results in Table 5-1 show a low recovery of the tracer. A way of avoiding this problem is by using the total proportionality factor determined from the mass of injected tracer and the pumping flowrate in the detection hole. This means that we force the mass balance to be obeyed.

The use of the total proportionality factor reduces the number of parameters to be determined by one. These results are shown in Table 5-1 and Figures 5-3 and 5-4. The values of the Peclet numbers, water residence times, and proportionality factors obtained in this fitting process will be used in the fit of the tracer test with sorbing tracer.

A low Peclet number is found in the last case. The one-dimensional model, which is used in these calculations, is a good approximation to the convergent radial flow when the Peclet number is large, Pe > 3 (Sauty, 1980). The results obtained using a low Peclet number are uncertain.

The ratio between the injection flowrate and the water flowrate pumped up is 0.104. This means that if the flow is evenly distributed in the plane of the fractures around the pumping hole, then the flow from the injection hole form a sector of 37° in a circle around the pumping hole. Then the experiments can not be defined as a tracer test with convergent flow. The actual experiment lies between a test with convergent flow and a dipole experiment. In a dipole experiment the injection and pumping flowrates are identical. This may, in part, explain the high dispersion of the breakthrough curve.

Fracture apertures were calculated from the fitted curves. Different fracture apertures may be defined and they are calculated using different data (See Section 4.1).

The water residence time, t_w, is determined from the tracer tests with nonsorbing tracer. The difference of pressure head, Δh, was directly measured during the experiments. The detailed flowrate Q through the fracture is difficult to determine. The total flowrate in the pumping hole is known however. The flowrate in the fractures through which the tracer flows is determined from hydraulic conductivity measurements and the total flowrate in the pumping hole. By assuming that the flowrate is evenly distributed over all the fracture, the flowrate along the tracer path is determined. The results are shown in Table 5-1.

The values of fracture apertures obtained for δ_f were high or very high, e.g., the model with two pathways shows an aperture as high as 22 mm. This is entirely unrealistic. This result is possibly due to the fit of the second curve giving a low Peclet number. The Peclet number and water residence time are inversely correlated.

In all the cases the value of δ_f is several orders of magnitude greater than the value of δ_l. This may be explained if we consider that the fracture aperture is not constant. The value of δ_f takes into account the average volume of the fracture, while δ_l takes into account the pressure drop along the direction of the flow. The pressure drop is caused, principally, by the constrictions in the direction of the flow.

Neither flow paths are known nor where the mixing between the injected tracer flow and the flow caused in the fracture by pumping in the withdrawal hole occurs. If the injected flow (0.01 l/min) moves with the same velocity as the total flow (0.096 l/min) and the fracture properties are the same everywhere, then the injection flow would represent the total flow. It would move in a sector 0.01/0.096 of the total arc. Equation (4.4) could then be used either with all the pumping flowrate and the full circle or the injection flowrate and the fraction of the circle which represents the injection arc.

In the extreme case we can envisage that the injection flowrate moves in the full circle except for a negligible portion where a major channel carries all the other flowrates to the pumping hole. Then the tracer residence time is representative of the tracer flowrate in all the fractures and a much

smaller aperture is needed to account for the tracer residence time. Figures for this minimum aperture are given in parenthesis in Table 5-1.

Table 5-1 Results for the nonsorbing tracer tritiated water. Advection-Dispersion model. Run B1N-B6N.

Case	(1)	(2)	(3)	(4)
Number of Pathways	1	2	1(a)	2(a)
Pe (1)	9.2±1.3	35.6±2.6	3.0±0.5	32.2±2.8
Pe (2)	-	2.9±0.3	-	1.4±0.1
t_w (1), h	430±25	292±2	861±62	298±3
t_w (2), h	-	1017±74	-	1936±130
rpf (1)	1.0	0.17	1.00	0.15
rpf (2)	-	0.83	-	0.85
δ_f (1), mm(b)	5.67	0.65	11.3	0.59
	(0.59)	(0.68)	(1.18)	(0.061)
δ_f (2), mm	-	11.1(1.15)	-	21.7(2.26)
δ_l (1), mm	0.011	0.014	0.008	0.014
δ_l (2), mm	-	0.007	-	0.005
δ_c (1), mm	0.131	0.073	0.131	0.070
δ_c (2), mm	-	0.123	-	0.124
Recovery				
at t=9240 h	0.48	0.76	1.00	0.98
at t= ∞	0.48	0.76	1.00	1.00
s/C_{max}	0.094	0.016	0.132	0.022
Figure	5-1	5-2	5-3	5-4

(a) Total proportionality factor determined from experimental data.

(b) The figures in parentheses give apertures based on the assumption that the injected flowrate travels to the pumping hole without dilution and uses the whole circle around the pumping hole. Dilution takes place in the pumping hole.

(__) Underlined values indicate that they were obtained in the fit.

5.2 A TEST OF THE INFLUENCE OF THE INJECTION PROCEDURE

In the previous analysis it was assumed that the injection was performed as an ideal pulse. The influence on the results of an injection that is not instantaneous is explored below. A volume of 0.5 l of groundwater containing the tracers was injected between the two packers. The injection of the tracers lasted about 1 hour. Prior to and after the tracer injection, groundwater was pumped down into the injection zone in order to develop a steady state flow into the fractures.

In the calculations the injection is considered as a pulse injection. The tracers are injected during a short interval of time. In practice, the injected tracer is mixed, to a certain degree, with the groundwater in the injection hole between the packers. The water volume between the packers in the injection hole is several times greater than the injected volume. The mixing with the water contained between the packers modifies the form of the injection. The concentration into the fractures will continuously change with the time.

In reality the injection process would lie between two limiting cases:

- plug flow in the hole without mixing
- injection hole acts as a well stirred tank.

The influence of the injection procedure will be studied by comparing breakthrough curves for both cases. The curve calculated in Table 5-1 (column 1) is based on plug flow in the injection hole. When the injection hole acts as a well stirred tank, breakthrough curves for different water volumes between the packers are calculated.

The total volume between the packers is 13.5 l. It is assumed that 50 % of this volume is occupied by the injection equipment. Then, the volume of water is about 6.25 l. The concentration of the tracer injected into the fracture may be expressed as

$$C_o = C'_o \frac{Vi}{V} e^{-\frac{Q}{V}t} \qquad (5.4)$$

where

C'_o = concentration of the injection into the fracture

C_o = concentration of the injection into the injection hole

V_i = volume of the injection in the injection hole

V = volume of the injection hole filled with water

Q = injection flow.

It is assumed that all the tracer is instantaneously injected to the water volume in the injection hole.

The analytical solution for a well stirred tank in the injection hole is found using the convolution integral. The concentration at the sampling hole may be written as

$$\frac{C}{C_o} = \frac{1}{2}\frac{V_i}{V}\exp\left(\frac{Pe}{2}\right)\int_o^{t_R}\frac{Pe^{1/2}}{\sqrt{\pi\,\xi^3}}\cdot$$

$$\exp\left[-\frac{Pe}{4\xi}-\frac{Pe\,\xi}{4}-\frac{Q}{V}t_o\,(t_R-\xi)\right]d\xi \qquad (5.5)$$

The results show that if the water volume is less than 10 l, then the injection may be considered as a pulse injection with plug flow in the injection hole. The injection procedure in this case has little influence on the result of the fit. This is because the residence time in the injection hole is much less than the water residence time in the fracture.

5.3 RESULTS FOR THE SORBING TRACER STRONTIUM

5.3.1. Use of no prior information

Fits were done including the three parameters for each pathway. The results show proportionality factors which are very different from the values obtained in the run with nonsorbing tracer. The proportionality factors obtained from the fits are very small due to the low recovery of the sorbing tracer. The recovery of the sorbing tracer strontium was as low as 6 % during the observation period (about 8700 hours).

In the experimental data for the strontium run, a peak was observed at a time of about 400 hours. Its arrival time was approximately equal to the arrival time for the nonsorbing tracer, tritiated water. One explanation for this first peak may be that some strontium is sorbed on particles or complexed by organics in the water and transported in one of these forms (Landström et al., 1983). This first peak was removed from the experimental data and new fits were made. The one pathway model showed identical results to those when the first peak was included. The proportionality factors are very small indicating that there is an important mechanism which is not accounted for in the model. In the next fits a specific loss factor is included. Possible causes of the loss will be discussed later.

5.3.2 Use of information from nonsorbing tracer

A fit was made using Peclet numbers, proportionality factors, and water residence times from the run with the nonsorbing tracer. The values in Table 5-1 are used. The fit is made for independent retardation factors in each pathway. Due to the very low recovery of the sorbing tracer a loss factor was included in the fit. The loss factor indicates how much of the tracer that will not be recovered even if the monitoring time continued on indefinitely. The recovery during the experiment was smaller because there was still tracer in the flowpath which had not yet arrived. The theoretical recovery is defined as (1-LF). The loss factor allows for calculating the recovery of the tracer if the time is long enough. The theoretical recovery is about 11 % of the injected tracer. This is the amount which the model predicts that will eventually be recovered. Eighty-nine percent of the injected strontium will never be recovered from this model.

The results are shown in Table 5-2 and Figures 5-5 and 5-6.

A fit was also made assuming that there is no loss and that all the strontium would eventually be recovered. This means that 100 % of the theoretical recovery is imposed on the fitted curve. The agreement with the experimental data then is very poor. The standard deviation of the fits s/C_{max} was 42 and 34% for one and two pathways, respectively. The tracer residence times in all the cases were greater than four times the observation time, which is unrealistic because this is well past the peak. Thus, this model is totally inadequate to explain the experimental data.

The low recovery of the sorbing tracer may be due to several causes:

- diffusion into the matrix of the rock
- precipitation
- irreversible sorption
- fast sorption and slow desorption
- large tracer residence times.

We will only test the first mechanism for which there is some independent data. Irreversible sorption, precipitation, fast sorption, and slow desorption may be modeled but due to the lack of independent data an unspecified loss factor will have to suffice at present.

Table 5-2 Results for the sorbing tracer strontium. Advection-Dispersion model. Run B1N-B6N. First peak removed from the experimental data.

Case	(1)	(2)
Number of Pathways	1	2
Pe (1)	3.0	32.2
Pe (2)	-	1.4
t_t (1), h	10610	5223
t_t (2), h	-	17220
rpf (1)	12.3	17.5
rpf (2)	-	8.9
Loss Factor	0.885	0.887
Recovery		
at t=8736 h	0.061	0.058
at t= ∞	0.115	0.113
s/C_{max}	0.16	0.11
Figure	5-5	5-6

([a]) Peclet numbers, water residence times, and proportionality factor from nonsorbing tracer test (Table 5-1).

(__) Underlined values indicate that they were obtained in the fit.

6 RESULTS OF THE FITTING PROCESS USING THE ADVECTION-DISPERSION-MATRIX DIFFUSION MODEL

The concentration at the outlet may be written as

$$C_f(t) = pf\ C(Pe,\ t_o,\ A,\ t) \tag{6.1}$$

For the nonsorbing tracer t_w is used instead of t_o. In these fits, the proportionality factor, pf, is determined from the injected tracer and the water flow. The hydraulic properties determined from the nonsorbing tracer test are used for the strontium test.

6.1 RESULTS FOR THE NONSORBING TRACER TRITIATED WATER

The experimental data were reduced from 89 to 31 points to shorten the computation time. Also from the reduction, a more even distribution of the experimental data was obtained. A fit was made including the three parameters. The proportionality factor is determined from the injected tracer and the pumping flowrate. The result of this fit is shown in Table 6-1 and Figure 6-1. The fit is good but the value of the A-parameter is very low. From this value of A it is possible to estimate the value of $(D_e \cdot K_d \cdot \rho_p)$. For a nonsorbing tracer R_a is equal to zero. Thus the fracture aperture used in the definition of the A-parameter in equation (3.11) may then be eliminated using equation (4.4). The A-parameter becomes

$$A = \frac{Q}{2\,(D_e\ K_d\ \rho_p)^{1/2}\ \pi\,(r_2^2 - r_1^2)}\ t_w \tag{6.2}$$

From equation (6.2) the value of the group $D_e \cdot K_d \cdot \rho_p$ may be determined once A is known. Assuming that all the flowrate arriving to the pumping hole (0.096

l/min) has the residence time t_w, a value of $8.0 \cdot 10^{-12}$ m^2/s is obtained for $D_e \cdot K_d \cdot \rho_p$. Since the tritiated water, which was used as a tracer, is nonsorbing then $K_d . \rho_p = \varepsilon_p$. The value of ε_p for intact granites may be expected to be on the order of 10^{-3} to 10^{-2}. This gives the effective diffusivity D_e in the range $8.0 \cdot 10^{-10}$ to $8.0 \cdot 10^{-9}$ m^2/s and the pore diffusivity D_p in the interval $8.0 \cdot 10^{-8}$ to $8.0 \cdot 10^{-6}$ m^2/s. However, these values are totally unrealistic since they are far larger than the diffusivity in unconfined water.

To test the sensitivity of the diffusivity on the results, a fit was made using a "reasonable" value of $D_e \cdot \varepsilon_p$ and fitting the other two remaining parameters. Q is taken to be the pumping flowrate.

The value of the effective diffusion coefficient for tritiated water in granite from the Studsvik area has not been determined. There are, however, data from other granites (Skagius and Neretnieks, 1986a). Calculations were done for two different values of $D_e \cdot \varepsilon_p$ ($6 \cdot 10^{-15}$ and $3 \cdot 10^{-16}$ m^2/s). The results are rather similar. The fit for $D_e \cdot \varepsilon_p = 6 \cdot 10^{-15}$ m^2/s is shown in Table 6-1 (case 2) and Figure 6-2. In this case the fit is poor. This result is similar to the value obtained using the hydrodynamic dispersion model without diffusion into the matrix. The interaction with the matrix is not large for this combination of parameter values.

In summary, when the Advection-Dispersion-matrix Diffusion model is used to fit the experimental data for tritiated water a low A-parameter is obtained. This value indicates a high interaction with the rock matrix. If all the pumping flowrate has a residence time t_w, a porosity of about 10 % is needed to explain this high interaction. Such a value of porosity is usually not found in granite. The porosity in granite close to the fracture may show a high value of about 3 % (Skagius and Neretnieks, 1986a). The high interaction may be explained only in part by a higher porosity for the granite near the fracture. Other mechanisms may exist which are not included in the model. Moreno et al. (1983) showed that the existence of zones of stagnant water may explain the tail of breakthrough curves in tracer tests with nonsorbing tracers. If the A-parameter is calculated assuming a value for

$D_e \cdot \varepsilon_p$ of $6 \cdot 10^{-15}$ m^2/s the results are almost similar to the value obtained with the dispersion model without diffusion. This means that values of $D_e \cdot \varepsilon_p$ of $6 \cdot 10^{-15}$ m^2/s or less give a negligible interaction with the rock matrix which is almost equivalent to the case without diffusion into the matrix.

If the injected flowrate with the tracer has transversed a large part of the flow path without mixing with the main flow (pumping flowrate), then the flowrate Q used in equation (6.2) should be closer to the injection flowrate. In this case the value of $D_e \cdot \varepsilon_p$ is $9.4 \cdot 10^{-14}$ m^2/s. This is about an order of magnitude larger than the measured values. Thus, in this case, even a high matrix diffusivity is needed to account for the interaction with the matrix.

The fracture aperture δ_f needed to account for the residence time of the injection flowrate is 0.22 mm instead of the 2.2 mm needed to account for the 9.6 times larger pumping flowrate. The larger aperture (2.2 mm) seems quite unreasonable. Such fracture openings are not observed over large distances.

Assuming that matrix diffusion is active with a $D_e \cdot \varepsilon_p$ = $6 \cdot 10^{-15}$ m^2/s (in the range of measured values) and that the residence time obtained in case (1) in Table 6-1 is correct, then the fracture aperture δ_1 of the flow path where the tracer flow has moved is 0.018 mm.

Table 6-1 Results for the nonsorbing tracer tritiated water. Advection-Dispersion-matrix Diffusion model. Run B1N-B6N.

Case	(1)	(2)
Pe	78.5(52.5-117)	3.09±0.83
t_w, h	167±14	840±104
A	388±43	$7.1 \cdot 10^4$
$pf \cdot 10^3$ [a]	8.16	8.16
δ_f, mm [b]	2.20(0.22)	11.1(1.15)
δ_1, mm	0.018	0.008
δ_c, mm	0.131	0.131
Recovery		
at t =9240 h	0.85	0.99
at t= ∞	1.00	1.00
s/C_{max}	0.04	0.13
Figure	6-1	6-2

[a] The proportionality factor is determined by forcing the recovery for $t_w \rightarrow \infty$ to become 100%.

[b] The figures in parentheses give apertures based on the assumption that the injected flowrate travels to the pumping hole without dilution and uses the whole circle around the pumping hole. Dilution takes place in the pumping hole.

(___) Underlined values indicate that they were obtained in the fit.

Case

(1) Fit using 3 parameters.

(2) Fit using 3 parameters. The value of A is calculated considering a nonsorbing tracer and $D_e \cdot \varepsilon_p = 6 \cdot 10^{-15}$ m²/s.

6.2 RESULTS FOR THE SORBING TRACER STRONTIUM

The experimental data for the sorbing tracer were reduced to a third in the same way as for the run with the nonsorbing tracer. The first peak at a time of about 400 hours was removed from the data. This was done because this peak obviously did not belong to either the same pathways or because a portion of the tracer did not have the same sorption properties.

In the first fit the Peclet number obtained in the run with the nonsorbing tracer (Table 6-1, column 1) was used. The results are shown in Table 6-2 (column 1) and Figure 6-3. The total predicted recovery is about 10 %.

Table 6-2, column 2 shows the results of the fit using a Peclet number from the nonsorbing tracer test when a value of $6 \cdot 10^{-15}$ m^2/s is used for $D_e \cdot \varepsilon_p$ (Table 6-1, column 2). The obtained A-parameter is characteristic of a nonsorbing species and the recovery is only about 10%. When a theoretical recovery of 100% is demanded (Table 6-2, column 3, the proportionality factor determined from the injected tracer) the fit is very poor.

The above attempts to fit the experimental data to models show that there is an unexplained (not modeled) loss of about 90 % of the strontium. Further it is evident that the fitting is very sensitive to both dispersion and matrix diffusion effects (cases 1 and 2). When low dispersion is forced upon the fit (case 1) the A-parameter decreases indicating that matrix diffusion and sorption effects may also explain the broadening of the curve to a large extent.

If a theoretical recovery of 100 % is demanded for the sorbing tracer the fitting process is very bad. In the run with a low Peclet number no agreement between the fitted curve and the experimental breakthrough curve is obtained. Matrix diffusion and reversible sorption within the rock matrix can not alone explain the low recovery during the observation time.

Table 6-2 Results for the sorbing tracer strontium. Advection-Dispersion-matrix Diffusion model. Run B1N-B6N.

Case	(1)	(2)	(3)
Pe	78.5	3.09	3.09
t_t	3449±394	9721±1500	3231(1105-9425)
A	3053±1255	$2.7\ 10^{10}$(a)	415(132-1298)
pf 10^3	0.796±.202	0.862±.117	8.16
R_a	20.6	11.6	3.85
Recovery			
at t=8736 h	0.049	0.061	0.064
at t= ∞	0.098	0.106	1.00
s/C_{max}	0.14	0.17	0.21
Figure	6-3	6-4	6-5

(a) Very large interval for 95 % confidence.
(__) Underlined values indicate that they were obtained in the fit.

Case
(1) Pe from nonsorbing tracer test (Table 6-1, column 1).
(2) Pe from nonsorbing tracer test (Table 6-1, column 2).
(3) Pe and pf from nonsorbing tracer test (Table 6-1, column 2).

6.3 RESULTS CONSIDERING FLOW THROUGH TWO PATHWAYS

Due to the difficulties to fit the experimental data for strontium with the Advection-Dispersion-matrix Diffusion model using one pathway, the model was extended to two pathways. Landström et al. (1983) pointed out that various pathways may exist between hole B1N and B6N. A model with two pathways including matrix diffusion needs the determination of 8 parameters. The use of so many parameters reduces the possibility of giving them a meaningful physical interpretation. For this reason the number of parameters is decreased. For the nonsorbing tracer the A-parameters are calculated assuming that the value of $D_e \cdot \varepsilon_p$ is known and the total proportionality factor is determined from the injected tracer flowrate. The Peclet numbers, water residence times, and one of the proportionality factors are determined by the fitting process. The results are shown in Table 6-3. The fit is very good. The results are similar to the results obtained with the AD-model, with two pathways. This means that the effect of the matrix is negligible for the nonsorbing tracer for the residence time, fracture aperture, and effective diffusivity which exist in these runs. This has been discussed above.

The fit for the sorbing tracer was made to investigate if the low recovery of the tracer strontium could be explained by diffusion into and sorption within the rock matrix from two pathways. A fit was made using the Peclet number from the nonsorbing tracer test. This gives a low theoretical recovery (7.3 %) and a very high A-parameter. The high A-parameter is due to that the breakthrough curve for the strontium is almost symmetrical with respect to the principal peak. This is characteristic for nonsorbing tracers.

In a second fit the proportionality factors and Peclet numbers from the nonsorbing tracer test were used. This means that a theoretical recovery on 100% was imposed on the fit. In this case pathway 2 which would carry 78 % of the tracer, has a tracer residence time of 16,930 hours. This residence time is twice the observation time. Moreover the fit is very poor.

The use of the Advection-Dispersion-matrix Diffusion model with two pathways does not improve the fit for the sorbing tracer strontium. When the proportionality factor is fitted the recovery is

very low and the A-parameter obtained in the fit is characteristic for nonsorbing tracer. If a recovery of 100 % is imposed, the fit is not good and the pathway with most of the flow shows a tracer residence time twice greater than the observation time. These results show that the breakthrough curve for strontium can not be explained for the ADD model using one or two pathways.

Table 6-3 Results for nonsorbing and sorbing tracers. Advection-Dispersion-matrix Diffusion model. Run B1N-B6N. Two pathways.

Case	Nonsorbing (1)	Sorbing (2)	Sorbing (3)
Pe (1)	38.7	38.7	38.7
Pe (2)	1.3	1.3	1.3
t_w (1), h	279	5226	2403
t_w (2), h	1950	11420	16930
A (1)	4243	$5.9\ 10^5$	1272
A (2)	$1.4\ 10^5$	$2.9\ 10^6$	5.49
pf (1) 10^3	1.46	0.22	1.46
pf (2) 10^3	6.70	0.38	6.70
Recovery			
at t=9240 h	0.97	-	-
at t=8736 h	-	0.05	0.06
at t= ∞	1.00	0.07	1.00
s/C_{max}	0.02	0.05	0.16

Case
(1) Fit for the nonsorbing tracer using 5 parameters. The A-parameter is calculated with $D_e \cdot \varepsilon_p = 6 \cdot 10^{-15}$ m^2/s.
(2) Fit for the sorbing tracer using 6 parameters. Pe's from nonsorbing tracer test.
(3) Fit for the sorbing tracer using 4 parameters. Pe's and pf's from nonsorbing tracer test.
(__) Underlined values indicate that they were obtained in the fit.

7 RESULTS OF THE FITTING PROCESS USING THE ADVECTION CHANNELING-MATRIX DIFFUSION MODEL

The concentration at the detection hole may be written as

$$C_f(t) = p_f\, C(\sigma, t_w, B, K_a, t)$$

for the nonsorbing tracer $K_a = 0$. The proportionality factor accounts for the dilution effect.

7.1 RESULTS FOR THE NONSORBING TRACER TRITIATED WATER

The experimental breakthrough curve for the tritiated water was fitted using three parameters. The proportionality factor was determined from the mass of tracer injected. The results are shown in Table 7-1. Using the pumping flowrate 0.096 l/min for Q and thus the larger aperture δ_f, the agreement is good but the value of the B-parameter is high. For a nonsorbing tracer the value of the B-parameter is expected to be 1-2 orders of magnitude smaller. $D_e \cdot \varepsilon_p$ may be directly calculated from the B-parameter, considering that tritiated water is a nonsorbing tracer ($K_d \cdot \rho_p = \varepsilon_p$). The value obtained for $D_e \cdot \varepsilon_p$ was $8.0 \cdot 10^{-12}$ m^2/s. This value is 2-3 orders of magnitude higher than the expected value for tritiated water. The A-parameter can directly be obtained from B with the following relation $A = R_a\delta/(2B)$. It is seen by comparison of Tables 7-1 and 6-1 that the A-values are practically the same.

A fit was also made setting the B-parameter to $D_e \cdot \varepsilon_p = 6 \cdot 10^{-15}$ m^2/s. In this case only two parameters were fitted (standard deviation in the lognormal distribution and mean water residence time). The fit was poor in this case (Table 7-1, case 2).

The results obtained with this model were similar to those obtained with the ADD model. Using the relation between σ and Pe (Moreno et al., 1985) it is found that the values of σ shown in Table 7-1 correspond to Peclet numbers of 85.6 and 3.35 for σ-values of 0.076 and 0.342, respectively. It is thus found that the residence times, dispersivities, matrix interaction parameters, and mean fracture apertures in both models are almost the same.

This model is similar to the ADD model. The difference between the two models is the manner in how they consider the spreading (dispersion) of the tracer. In the ACD model the fracture is represented by a large number of independent channels with different apertures. So, it is not possible to distinguish the dispersion mechanism since both models fit the same experimental data in a similar manner (Moreno et al., 1985).

Table 7-1 Results for the nonsorbing tracer tritiated water. Advection-Channeling-matrix Diffusion model. Run B1N-B6N.

Case	(1)	(2)
σ	0.076	0.342
$\bar{t}_w$, h	181	873
B	$2.82\ 10^{-6}$	$7.75 \cdot 10^{-8}$
$pf \cdot 10^3$	8.16	8.16
δ_f mm [a]	2.38 (0.25)	11.5 (1.20)
δ_l, mm	0.017	0.008
δ_c, mm	0.131	0.131
Recovery		
at t=9240 h	0.85	0.99
at t= ∞	1.00	1.00
s/C_{max}	0.04	0.15
Figure	7-1	7-2

[a] The figures in parentheses give apertures based on the assumption that the injected flowrate travels to the pumping hole without dilution and uses the whole circle around the pumping hole. Dilution takes place in the pumping hole.

(__) Underlined values indicate that they were obtained in the fit.

Case

(1) Fit using 3 parameters. Pf is determined from experimental data.

(2) Fit using 2 parameters. Pf is determined from experimental data and B-parameter is calculated considering nonsorbing tracer ($K_d \cdot \rho_p = \varepsilon_p$) and $D_e \cdot \varepsilon_p = 6 \cdot 10^{-15}$ m^2/s.

7.2 RESULTS FOR THE SORBING TRACER STRONTIUM

The first peak at a time of about 400 hours was removed from the experimental breakthrough curve. The standard deviation in the lognormal distribution and mean water residence time determined for the nonsorbing tracer (Table 7-1, column 1) were used to fit the tracer test with strontium. The B-parameter and the surface sorption coefficient are determined in the fitting process. The proportionality factor is included in the fit. This is equivalent to the use of a recovery or loss factor. The results are shown in Table 7-2.

New fits are made using the standard deviation in the lognormal distribution and the mean water residence time for the nonsorbing tracer test shown in Table 7-2, column 2. In both cases the fits are poor.

It is not possible to compare these results with the values obtained with the ADD model due to the poor fits obtained for the strontium tracer test. A rough comparison is made for the fit shown in Table 7-2 (column 1) with the fit in Table 6-2 (column 1). In the ACD model the channels with smaller apertures show a greater retardation factor than the wider channels. This produces a larger dispersion of the outlet concentration. This dispersion is compensated in the ADD model by a larger diffusion into the matrix. This increases the retardation factor in the ACD model. These relationships were also observed in a tracer test in natural fractures in the laboratory (Moreno et al., 1985).

Table 7-2 Results for the sorbing tracer strontium. Advection-Channeling matrix Diffusion model. Run B1N-B6N.

Case	(1)	(2)	(3)
σ	0.076	0.342	0.342
$\bar{t}_w$, h	181	873	873
B	$\underline{4.3\ 10^{-6}}$	$\underline{2.7\ 10^{-5}}$	$\underline{6.7\ 10^{-5}}$
pf.10^3	$\underline{0.58}$	$\underline{3.23}$	8.16
K_a, m	$\underline{2.7\ 10^{-2}}$	$\underline{0.13}$	$\underline{0.18}$
Recovery			
at t=8736 h	0.05	0.06	0.06
at t= ∞	0.07	0.40	1.00
s/C_{max}	0.11	0.20	0.21
Figure	7-3	7-4	7-5

Case

(1) Standard deviation in the lognormal distribution and mean water residence time from the nonsorbing tracer test (Table 7-1, column 1).

(2) Standard deviation in the lognormal distribution and mean water residence time from the nonsorbing tracer test (Table 7-1, column 1).

(3) Standard deviation in the lognormal distribution mean water residence time and proportionality factor from the nonsorbing tracer test (Table 7-1, column 2).

(__) Underlined values indicate that they were obtained in the fit.

8 RESULTS FOR THE TRACER TEST B5N-B6N

The tracer test B5N-B6N was fitted using the three models (AD, ADD, and ACD models). The experimental breakthrough curves showed a recovery of 96 % for tritiated water and 18 % for strontium during the observation time.

The breakthrough curve for the nonsorbing tracer showed a high dispersion (long tail). The experimental curve for the sorbing tracer showed a first peak with an arrival time similar to the arrival time for the nonsorbing tracer. After the second peak (or the main peak) the concentration decreased to a low value. But at the end of the observation time the concentration in the detection hole increased again. The breakthrough curves for tritiated water and strontium are shown in Figures 2-4 and 2-5, respectively.

8.1 RESULTS FOR THE FIT USING THE ADVECTION-DISPERSION MODEL

The experimental data were fitted using the AD model with one and two pathways. The total proportionality factor was determined from the experimental data.

For the nonsorbing tracers the fit was good even when one pathway was used to fit the experimental data. When two pathways were used the results showed that 99 % of the tracer was transported by one of the pathways. This pathway has similar properties as those obtained using one pathway. The results are shown in Table 8-1 and Figures 8-1 and 8-2.

In both cases the main pathway shows a low Peclet number (0.7 and 0.8). The model used is not quite applicable when the Peclet number is smaller than 3 (Sauty, 1980). For this reason the results presented in Table 8-1 are very uncertain.

The results for the nonsorbing tracer showed values for the dispersion which are unusual if we assume that the dispersion is caused by the variations of velocity due to the roughness of the fracture. A reason for this high dispersion may be the existence of a large number of pathways with very different

velocities. Another explanation may be that the injection found a zone with "great" lakes in which the tracer is well mixed and from which it is transported by some other pathways to the pumping hole.

The apertures calculated from the water flowrate and water residence times (δ_f) were unrealistic large. This would occur if there is a strong uneven distribution at the collection hole. The tracer then would travel with a long residence time in a small portion of the flow whereas the main flowrate travels along another flowpath with a much higher velocity. Since the model implicity assumes that all flowpaths to the collection hole have equal properties, the residence time for the large flowrate is set equal to that "measured" by the tracer.

The recovery in the test with the sorbing tracer was about 18 % during the observation time (8,727 hours). The model with two pathways was used because the experimental breakthrough curve shows 2 peaks. First, a fit was made including the three parameters for each pathway. The results showed extremely small values for the Peclet numbers. For one pathway this parameter was much smaller than 0.1. The proportionality factor is smaller than the values obtained for the nonsorbing tracer due to the low recovery of strontium.

A new fit was made using the Peclet numbers and proportionality factors determined for the nonsorbing tracer. A loss factor was included in the fit due to the low recovery of the tracer strontium. The results are shown in Table 8-1 and Figure 8-3. The loss factor is 0.51 when 2 pathways are used which means that 49 % of the injected tracer should have been carried in the observation hole if the test was run for a very long time. The second pathway shows a tracer residence time of 31.580 hours. This value is about 4 times the observation time. If the tracer test for the sorbing tracer is adequately modeled by the Advection-Dispersion model, the only way to explain the low recovery is to assume that the retardation is very high. Most of the injected tracer would come to the observation hole after a time of 8,727 hours. This is supported by the increase of the outlet concentration observed between 7,000 hours and the last observation (8,727 hours).

Table 8-1 Results for the nonsorbing and sorbing tracers. Advection-Dispersion model. Run B5N-B6N. Total proportionality factor determined from experimental data.

Tracer	nonsorbing	nonsorbing	sorbing[b]
Number of Pathways	1	2	2
Pe (1)	0.7±0.1	11.8±7	11.8
Pe (2)	-	0.8±0.1	0.8
t_w (1), h	1200±92	38±5	-
t_w (2), h	-	1119±51	-
t_w (1), h	-	-	299
t_w (2), h	-	-	31580
t_w (1), h	-	-	7.9
t_w (2), h	-	-	28.2
rpf (1)	1.00	0.01	0.01
rpf (2)	-	0.99	0.99
δ_f (1), mm[a]	90.4 (0.88)	0.03 (0.0003)	-
δ_f (2), mm	-	83.4 (0.83)	-
δ_l (1), mm	0.009	0.052	-
δ_l (2), mm	-	0.010	-
δ_c (1), mm	0.165	0.035	-
δ_c (2), mm	-	0.164	-
Recovery			
at t=3960 h	0.94	0.95	0.17
at t= ∞	1.00	1.00	0.49
s/C_{max}	0.04	0.02	0.41
Figure	8-1	8-2	8-3

([a]) The figures in parentheses give apertures based on the assumption that the injected flowrate travels to the pumping hole without dilution and uses the whole circle around the pumping hole. Dilution takes place in the pumping hole.

([b]) Pe and pf determined from nonsorbing tracer test.

(__) Underlined values indicate that they were obtained in the fit.

8.2 RESULTS FOR THE FIT USING THE ADVECTION-DISPERSION-MATRIX DIFFUSION MODEL

When the three parameters were fitted using the ADD model the agreement was good for the nonsorbing tracer tritiated water. The proportionality factor was determined from the injected tracer and the flowrate. The value obtained for the Peclet number was very low. For this reason the results of the fit are uncertain.

The fit was also good when the A-parameter was determined from laboratory data, flowrate, and residence time. The results, in both cases, are rather similar because the breakthrough curve obtained in this test is characteristic for a tracer test with very high dispersion and without diffusion into the matrix. The tail of the curve is explained by a very high dispersion. The results are identical to the values obtained with the Advection-dispersion model. The results are shown in Table 8-2 and Figures 8-4 and 8-5.

This model could not fit the experimental data for strontium because the breakthrough curve had two peaks and possibly a third peak and this model uses only one pathway.

Table 8-2 Results for the nonsorbing tracer tritiated water. Advection-Dispersion-matrix Diffusion model. Run B5N-B6N.

Case	(1)	(2)
Pe	0.72(0.37-1.41)	0.73±0.08
t_w, h	1210(635-2305)	1203±98
A	$1.1\ 10^7$[a]	$5.4 \cdot 10^5$
$pf \cdot 10^3$	8.16	8.16
δ_f, mm[b]	91.1 (0.89)	90.6 (0.89)
δ_1, mm	0.009	0.009
δ_c, mm	0.165	0.165
Recovery		
at t=3960 h	0.93	0.93
at t= ∞	1.00	1.00
s/C_{max}	0.03	0.03
Figure	8-4	8-5

([a]) Very large interval for 95 % confidence.

([b]) The figures in parentheses give apertures based on the assumption that the injected flowrate travels to the pumping hole without dilution and uses the whole circle around the pumping hole. Dilution takes place in the pumping hole.

(__) Underlined values indicate that they were obtained in the fit.

Case

(1) Fit using 3 parameters. Pf is determined from the experimental data.

(2) Fit using 2 parameters. Pf is determined from experimental data and the value of A is calculated with $D_e \cdot \varepsilon_p = 6 \cdot 10^{-15}$ m^2/s.

8.3 RESULTS FOR THE FIT USING THE ADVECTION-CHANNELING-MATRIX DIFFUSION MODEL

Two fits were made for the nonsorbing tracer tritiated water. The breakthrough curves were fitted using the proportionality factor determined from the injected tracer. In the second fit the B-parameter was calculated with $D_e.\varepsilon_p = 6 \cdot 10^{-15}$ m^2/s. The results are shown in Table 8-3. The two fits present a high value for the standard deviation of the fracture aperture distribution. This is in agreement with the low values of the Peclet number obtained when this tracer test is fitted using the ADD model. The fits are good.

The mean water residence time for the ACD model were less than the values obtained with the ADD model. This is because that in the ACD model no dispersion is assumed in the channels. The differences in the water residence times are greater in the first fit, when the ADD model has a very low Peclet number.

The breakthrough curve with two or three peaks can not be fitted with this model.

Table 8-3 Results for the nonsorbing tracer tritiated water. Advection-Channeling-matrix Diffusion model. Run B5N-B6N.

Case	(1)	(2)
σ	0.435	0.508
$\bar{t}_w$, h	657	1012
B	$9.31\ 10^{-6}$	$7.75 \cdot 10^{-8}$
$pf \cdot 10^3$	8.16	8.16
δ_f, mm[a]	45.6 (0.45)	70.3 (0.69)
δ_l, mm	0.012	0.010
δ_c, mm	0.165	0.165
Recovery		
at t=3960 h	0.86	0.98
at t= ∞	1.00	1.00
s/C_{max}	0.03	0.05
Figure	8-6	8-7

([a]) The figures in parentheses give apertures based on the assumption that the injected flowrate travels to the pumping hole without dilution and uses the whole circle around the pumping hole. Dilution takes place in the pumping hole.

(__) Underlined values indicate that they were obtained in the fit.

Case

(1) Fit using 3 parameters. Pf is determined from experimental data.

(2) Fit using 2 parameters. B-parameter is calculated using $D_e \cdot \varepsilon_p = 6 \cdot 10^{-15}$ m^2/s and pf is determined from experimental data.

9 SUMMARY OF RESULTS AND DISCUSSION

It is clear that none of the models have been validated. The runs with the nonsorbing tracers in both pathways have very long tails which indicate either very strong dispersion, channeling, or interaction with stagnant pools of water. Matrix diffusion can play some role but is not a dominating effect. The mechanisms cannot be distinguished from each other with the information available.

One effect is evident from the evaluated fracture aperture data. In both tests the tracer must have been injected in a minor pathway. The residence time for the tracer solution which was injected with a flowrate of about 0.01 l/min cannot be equal to the residence time of the main water flowrate in the collection hole (0.096 and 1.02 l/min) because this leads to unacceptably large fracture apertures: 2.2 mm in pathway B1N-B6N and 45 to 90 mm in pathway B5N-B6N. These apertures should be interpreted in the following way. They constitute the void needed for the water flowrate to be able to reside during the residence time of the water. Fracture apertures of this size are not known to exist in practice. These figures are instead indications of strong channeling. The tracer flowrate may have been injected in a channel (system) with slowly moving water. Fast pathways carry the main stream of water to the collection hole where the waters from the paths mix. Figure 9-1 illustrates how the injection flowrate spreads into one channel system and that the main flowrate comes from another system. It is also illustrated that a partial dipole system may develop.

If the area covered by the injection flowrate is large it suffices to have a small aperture in the fracture. One extreme case is if the injection flowrate spreads out evenly over the fracture at a distance equal to the distance between the holes before it is drawn into the pumping hole. The fracture aperture needed to give the small injection flowrate the residence time is then accordingly smaller (9.6 and 102 times). The apertures become 0.23 to 0.25 mm instead of 2.2 to 2.4 mm for the B1N injection and 0.47 to 0.93 mm instead of 46 to 91 mm for the B5N injection. The smaller values seem to be more reasonable.

The fairly high temperature of the pumped water indicates that we probably have a main flow from

depths of 300-400 m and that the injection fracture constitutes a minor flow path

The fracture apertures δ_c obtained using the cubic law assumption are 0.13 and 0.17 mm. The apertures δ_l, which are based on the assumption that the measured residence time and pressure drop can be used to evaluate an aperture of a parallel slit, are 0.008 and 0.009 mm for the two pathways.

We conclude that it is not possible to determine a single value of the fracture aperture from the data obtained in this experiment. The widely differing results indicate that there are different pathways (channels) with widely different properties. The very low Peclet numbers (0.7-3), which were obtained in many fits, indicate that other effects than what is usually included in the term "hydrodynamic dispersion" are active. In the pathway B5N-B6N the Peclet number 0.7 indicates a dispersion length larger than the travel distance. This has little meaning and is an indication that the tracer has been transported by different pathways.

If the fractures have so widely different properties as these results indicate, then the techniques used in this experiment are not suitable to determine fracture aperture data to be used for the prediction of the movement of sorbing tracers. In case there is only surface sorption to retard the sorbing tracer, the retardation factor is

$$R_a = 1 + 2\ K_a / \delta_f$$

For most of the nuclides of interest the term $2 \cdot K_a/\delta_f$ is much greater than 1. Therefore, the surface retardation factor R_a is inversely proportional to δ_f. As in this case the residence time of the water is known, but we cannot predict the residence time of the strontium better than we know the aperture. The inaccuracy involved is a factor of about 10-100.

If matrix diffusion and bulk sorption are active, in addition to surface sorption, then the inaccuracies in predicting the sorbing tracer movement are even larger.

The strange behavior of the sorbing tracer showing a first peak, a second peak, and a large "loss" or very late arrival would be expected if there are large variations in the properties of the different pathways.

It cannot be excluded that all the models used may be applicable in individual pathways. The possible presence of a multitude of pathways with different and unknown properties has made it impossible to validate any of the models. The unknown pathways also make difficult (impossible) to ascertain the boundary conditions in each pathway. Figure 9-1 illustrates the difficulty of determining the number, length, and other properties of the channels.

To better utilize the results from this kind of tracer test it is necessary to have additional information of the properties of channels in fractures and fracture systems. Even so it seems that a straightforward evaluation of this kind of test may be difficult.

An alternative test method, the dipole test, may circumvent one of the main difficulties of this test. In this type of test the traced water injection rate is large and the pumping rate is equally large so that these flows dominate the flowrate in the system. The flowrate and its residence time distribution is then known. Although the test will not be a real dipole test in a fracture with varying properties, this procedure will at least eliminate one of the main drawbacks of the present test, namely the fact that the residence time of the main flowrate is not known.

The experimental recovery for the nonsorbing tracer tritiated water was 93 and 96 % in the runs B1N-B6N and B5N-B6N, respectively. The recoveries for the sorbing tracer strontium were very small. About 6 and 18 % of the tracer injected was recovered in the runs B1N-B6N and B5N-B6N, respectively. Small recoveries have been observed in other tracer test in situ. Klockars and Gustafsson (1981, 1984) reported recovery of 60 % for a tracer test with strontium in Finnsjön, with injection during 350 hours.

The low recovery of the sorbing tracer test analysed in this report may be caused by:

- irreversible sorption

- fast sorption and slow desorption

- large tracer residence time in some pathways.

In a water transmitting fracture of the core-drilled borehole the main coating mineral was smectite. This mineral has a high sorption coefficient for strontium. The occurrence of smectite in the injection fracture could thus partly explain the low recovery.

When the experimental equipment was dismounted ^{134}Cs activity was observed on the material within the injection volume (^{85}Sr had completely decayed). On the plastic tube a coating had developed during the experiment time mostly containing Fe but also Ca and S. The coating was analyzed for ^{134}Cs and it was found that about 5 % of the injected amount of ^{134}Cs had been sorbed on the coating. Whether part of ^{85}Sr was also sorbed can not be established.

From the breakthrough curves for strontium we can not give a reasonable explanation for the low recovery. The tests were stopped after about 8700 hours. The assumption of large retardation for the tracer strontium is supported by the increase of the outlet concentration observed in the run B5N-B6N for time large than about 7000 hours.

Laboratory experiments are required to study the kinetics of the sorption reaction. In this report it is assumed that the sorption reaction is reversible and instantaneous. Instantaneous means in this case that its time constant is negligible compared to the diffusion into the rock matrix and the water residence time. Laboratory experiments indicate that this is the case (Skagius, 1986). Reactions of strontium with other species in the groundwater and the fracture would need to be studied (e.g., formation of colloides).

When the proportionality factor is included in the fit, in general, the fitted curves showed a recovery of the tracer far from the observed recovery. To improve the fitting process two methods may be used:

- Calculation of the total proportionality factors from the experimental data (injected tracer). The curve shows a 100 % recovery for an infinite observation time.

- Comparing the recovery of the fitted curve with the experimental curve and modifying the proportionality factors. In this case the fitted curve shows the same recovery as the experimental curve during the observation time.

In the calculations done in this report the first method was chosen. The second method is an alternative when the mass of tracer injected is unknown or when only a part of the tracer comes to the detection hole.

The tracer tests with the nonsorbing tracer showed a high dispersion. The concentration increased to a maximum very fast, afterwards it decreased slowly showing a long tail. In run B5N-B6N the tail of the curve was very large and the dispersion obtained in the fit was very high - the Peclet number was less than 1.0. This could be explained by the presence of a large number of pathways with different residence times and lengths. Another explanation could be the existence of large "lakes" in the fracture where the tracer is well mixed. From these lakes the tracer could be transported to the pumping hole by means of one or several channels.

The AD and ADD models describe the water and tracer transport as occurring through a very thin two-dimensional porous bed. In the ACD model it is assumed that the water flows through a bundle of channels with different apertures. Each channel has a constant aperture. In the experimental measurements of the fracture apertures it was found that the apertures vary strongly along the fracture. Considering that this variation in the fracture aperture exists in the direction longitudinal and transversal to the main water flow, zones with low and high permeability will exist in the plane of the fracture. Water will be transported mainly through the channels which have high permeability. A network of channels will form in the plane of the fracture. The water flowrate in the channels will be determined by the constrictions in the channels. The channels will have different volumes, lengths, and residence times. Zones with stagnant water may exist in the fracture into which the tracer may diffuse by diffusion.

NOTATION

A	parameter defined in eq. (3.11)	
B	parameter defined in eq. (3.13)	
C_f	concentration in the liquid in the fracture	mol/m^3
C_m	concentration in the solid	mol/kg
C_p	concentration in the liquid in the pores	mol/m^3
C_s	concentration on the surface of the solid	mol/m^2
D_e	effective diffusivity into the rock	m^2/s
D_L	dispersion coefficient	m^2/s
h	hydraulic head	m
K_a	surface sorption coefficient	m
K_d	mass sorption coefficient	m^3/kg
K_{pf}	hydraulic conductivity of fracture	m/s
L	length of flow path	m
m	mass of tracer injected	mol
pf	proportionality factor	
Pe	peclet number	
Q	flowrate	m^3/s
r	radial distance	m
R_a	surface retardation factor in the channel	
rpf	relative proportionality factor	
s	standard deviation in the fit	
t	time	s
t_o	tracer residence time	s
t_w	water residence time	s
U_f	water velocity	m/s
V	volume of the fracture	m^3
x	distance in the direction of flow	m
z	distance into rock matrix	m
δ	fracture aperture in the channel in the fracture	m
ε_p	porosity of rock matrix	
λ	parameter defined in eq. (3.11)	
μ	log mean aperture	
ρ_p	density of rock matrix	kg/m^3
σ	standard deviation in the lognormal distribution	
υ	kinematic viscosity	m^2/s

REFERENCES

Abelin, H., I. Neretnieks, S. Tunbrant, and L. Moreno: "Final Report of the migration in a single fracture. Experimental results and evaluation," Stripa Project, TR 85-03, Stockholm, (1985).

Andersson, K., B. Torstenfelt, and B. Allard: "Sorption of radionuclides in geologic systems," KBS TR 83-63, Nuclear Fuel Safety Project, Stockholm (1983).

Andersson, P, and C.E. Klockars: "Hydrogeological investigations and tracer test in a well defined rock mass in the Stripa mine," SKB TR 85-12, Nuclear Fuel Safety Project, Stockholm (1985).

Carslaw, H.S., and J.C. Jaeger: "Conduction of heat in solids," 2nd ed., Oxford University Press, New York (1959).

Gustafsson, E., and C.E. Klockars: "Studies on groundwater transport in fractured crystalline rock under controlled conditions using non-radioactive tracers," KBS TR 81-07, Nuclear Fuel Safety Project, Stockholm (1981).

Gustafsson, E., and C.E. Klockars: "Study of strontium and cesium migration in fractured crystalline rock," KBS TR 84-07, Nuclear Fuel Safety Project, Stockholm (1984).

Landström, O., C.E. Klockars, K.E. Holmberg, and S. Westerberg: "In situ experiments on nuclide migration in fractured crystalline rocks," KBS TR 110, Nuclear Fuel Safety Project, Stockholm (1978).

Landström, O., C.E. Klockars, O. Persson, K. Andersson, B. Torstenfelt, B. Allard, E.L. Tullborg, and S.A. Larsson: "Migration experiments in Studsvik," KBS TR 83-18, Nuclear Fuel Safety Project, Stockholm (1983).

Lenda, A., and A. Zuber: "Tracer dispersion in ground water experiments," Proceedings of a symposium organized by IAEA, Vienna (1970).

Maloszewski, P., and A. Zuber: "On the theory of tracer experiments in fissured rocks with a porous matrix," Institute of Nuclear Physics, Rep 1244 AP, Cracow, Poland (1984).

Moreno, L., I. Neretnieks, and K.E. Klockars: "Evaluation of some tracer tests in the granite rock at Finnsjön," KBS TR 83-38, Nuclear Fuel Safety Project, Stockholm (1983).

Moreno, L., I. Neretnieks, and T. Eriksen: "Analysis of some laboratory tracer runs in natural fractures," Water Resour. Res., 21 951-958 (1985).

Neretnieks, I., T. Eriksen, and P. Tähtinen: "Tracer Movement in a Single fissure in Granitic Rock: Some Experimental Results and Their Interpretation," Water Resour. Res., Vol 18, 849 (1982).

Sauty, J.P.: "An analysis of hydrodispersive transfer in aquifers," Water Resour. Res., Vol 16, 145-58 (1980).

Skagius, K., G. Svedberg, and I. Neretnieks: "A study of strontium and cesium sorption on granite," Nuclear Technology, 59, 302-313 (1982).

Skagius, K.: "Diffusion of dissolved species in the matrix of some swedish crystalline rocks," Ph. D. thesis, Dept. Chemical Engineering, Royal Institute of Technology, Stckholm, Sweden, (1986).

Skagius, K., and I. Neretnieks: "Porosities and diffusivities of some nonsorbing species in crystalline rocks," Water Resour. Res., 22, 389-398 (1986a).

Skagius, K., and I. Neretnieks: "Diffusivity measurements and electrical resistivity measurements in rock samples under mechanical stress," Water Resour. Res., 22, 570-580 (1986b).

Skagius, K., and I. Neretnieks: "Measurements of cesium and strontium diffusion in biotite gneiss," Water Resour. Res., in print, (1988).

Snow, D.T.: "The frequency and apertures of fractures in rock," Int. J. Rock. Mech. Min. Sci., vol. 7, 23 (1970).

Tang, G.H., E.O. Frind, and E.A. Sudicky: "Contaminant Transport in Fractured Porous Media. An Analytical Solution for a Single Fracture," Water Resour. Res., Vol 17, 555 (1981).

FIGURES

Figure 6-6 Curve fitted using the ADD model with two pathways with the A-parameter determined using $D_e \cdot \varepsilon_p = 0.006 \cdot 10^{-12}$ m^2/s and the total proportionality factor determined from experimental data. Run B1N-B6N for the nonsorbing tracer tritiated water.

Figure 6-7 Curve fitted using the ADD model with two pathways with Peclet numbers from nonsorbing tracer test. Run B1N-B6N for the sorbing tracer strontium.

Figure 6-8 Curve fitted using the ADD model with two pathways with Peclet numbers and proportionality factors from nonsorbing tracer test. Run B1N-B6N for the sorbing tracer strontium.

Figure 7-1 Curve fitted using the ACD model with the proportionality factor determined from experimental data. Run B1N-B6N for the nonsorbing tracer tritiated water.

Figure 7-2 Curve fitted using the ACD model with the B-parameter determined using $D_e \cdot \varepsilon_p = 0.006 \cdot 10^{-12}$ m^2/s and the proportionality factor determined from experimental data. Run B1N-B6N for the nonsorbing tracer tritiated water.

Figure 7-3 Curve fitted using the ACD model with the standard deviation in the lognormal distribution from the nonsorbing tracer test (Table 7-1, column 1). Run B1N-B6N for the sorbing tracer strontium.

Figure 7-4 Curve fitted using the ACD model with the standard deviation in the lognormal distribution from nonsorbing tracer test (Table 7-1, column 2). Run B1N-B6N for the sorbing tracer strontium.

Figure 7-5 Curve fitted using the ACD model with the standard deviation in the lognormal distribution and proportionality factor from nonsorbing tracer test (Table 7-1, column 2). Run B1N-B6N for the sorbing tracer strontium.

Figure 8-1 Curve fitted using the AD model with one pathway with total proportionality factor determined from the experimental data. Run B5N-B6N for the nonsorbing tracer tritiated water.

Figure 8-2 Curve fitted using the AD model with two pathways with total proportionality factor determined from the experimental data. Run B5N-B6N for the nonsorbing tracer tritiated water.

Figure 8-3 Curve fitted using the AD model with two pathways with Peclet numbers and proportionality factors from nonsorbing tracer test. Fit includes tracer residence times and loss factor. Run B5N-B6N for the sorbing tracer strontium.

Figure 8-4 Curve fitted using the ADD model with the proportionality factor determined from experimental data. Run B5N-B6N for the nonsorbing tracer tritiated water.

Figure 8-5 Curve fitted using the ADD model with the A-parameter determined using $D_e \cdot \varepsilon_p = 0.006 \cdot 10^{-12}$ m^2/s and the proportionality factor determined from experimental data. Run B5N-B6N for the nonsorbing tracer tritiated water.

Figure 8-6 Curve fitted using the ACD model with the proportionality factor determined from experimental data. Run B5N-B6N for the nonsorbing tracer tritiated water.

Figure 8-7 Curve fitted using the ACD model with the B-parameter determined using $D_e \cdot \varepsilon_p = 0.006 \cdot 10^{-12}$ m^2/s and the proportionality factor determined from experimental data. Run B5N-B6N for the nonsorbing tracer tritiated water.

Figure 9-1 Possible flow situation into one channel system.

FIGURES

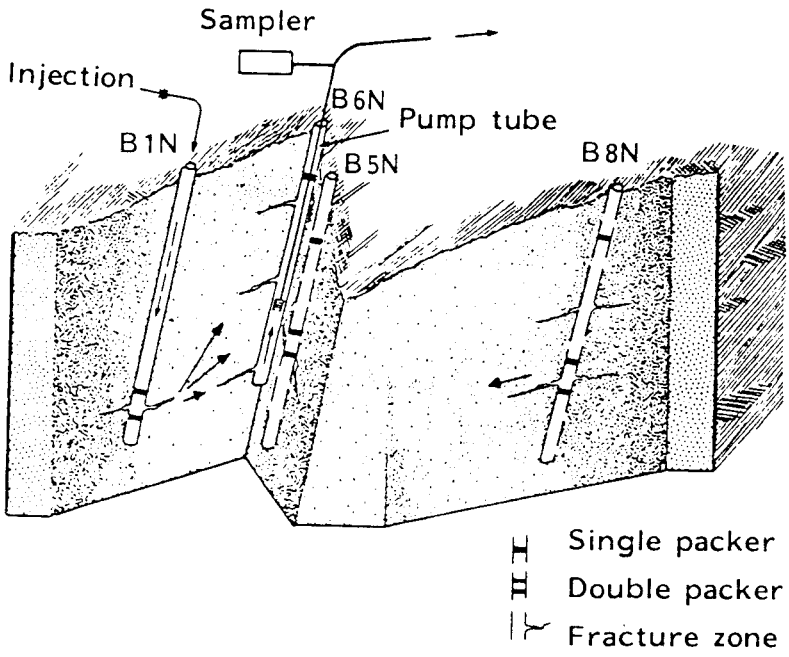

Figure 2-1 Cutaway view of the in situ test site.

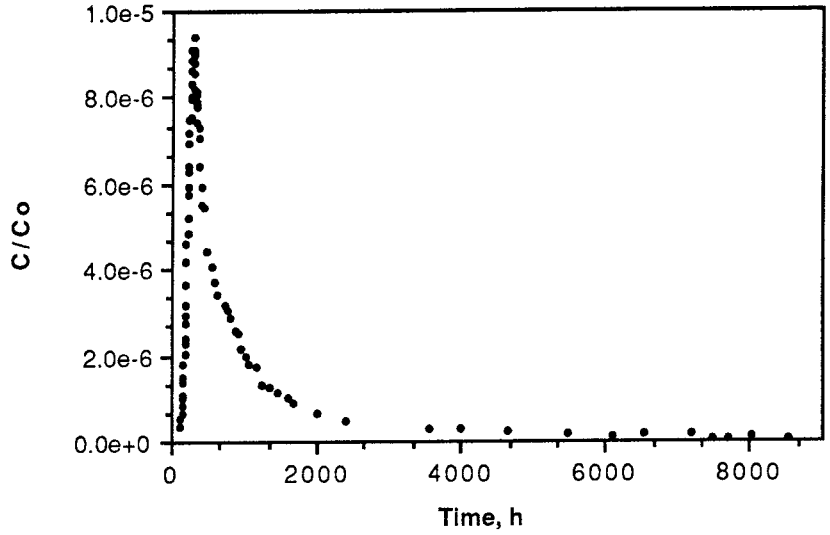

Figure 2-2 Experimental breakthrough curve for tritiated water for the run B1N-B6N.

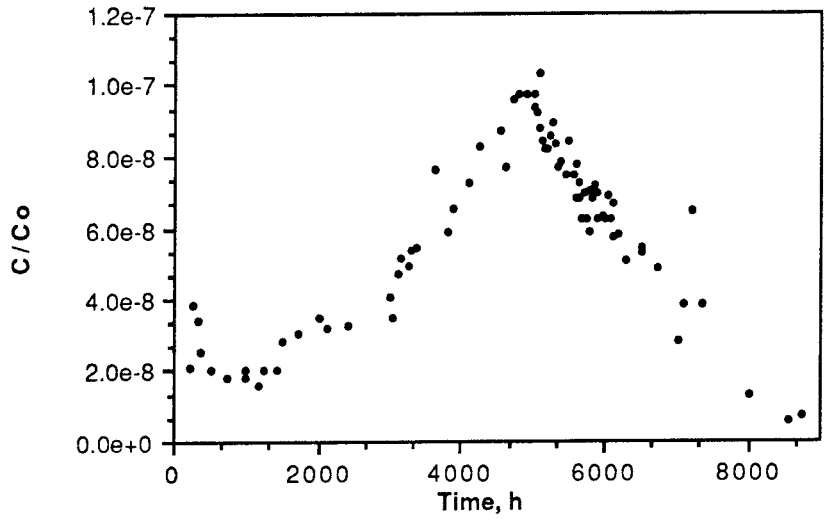

Figure 2-3 Experimental breakthrough curve for strontium for the run B1N-B6N.

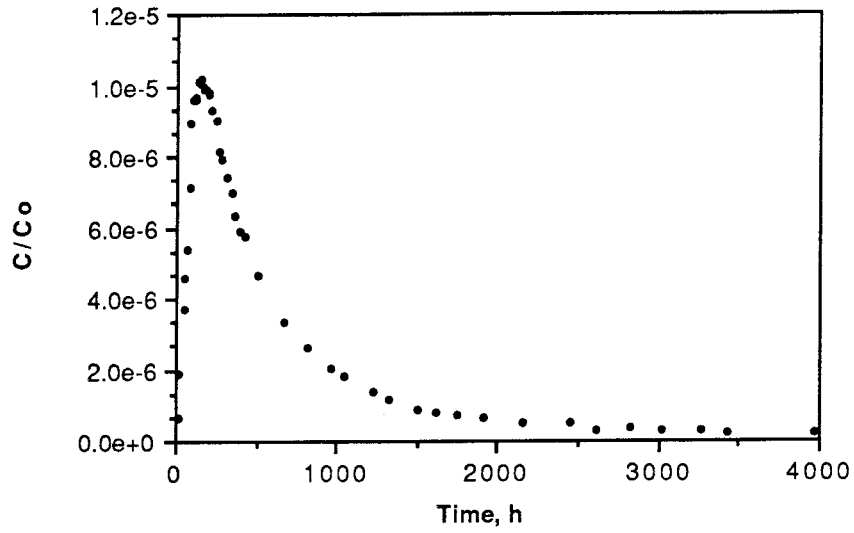

Figure 2-4 Experimental breakthrough curve for tritiated water for the run B5N-B6N.

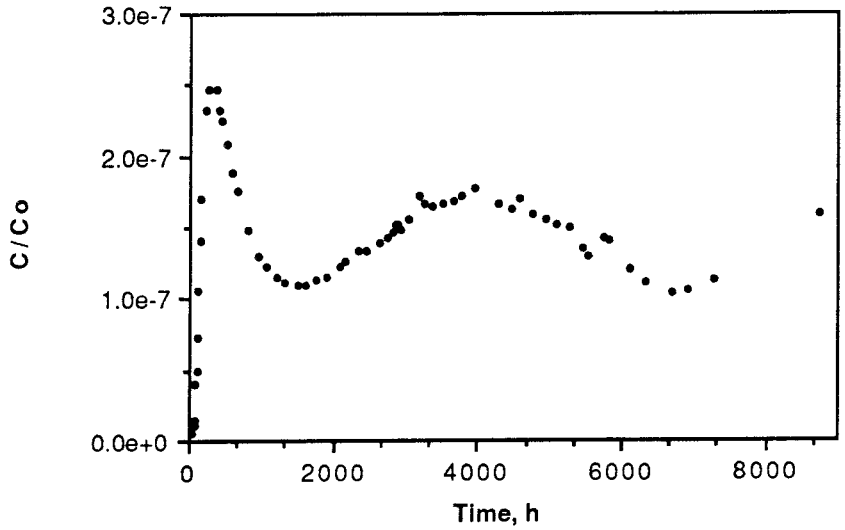

Figure 2-5 Experimental breakthrough curve for strontium for the run B5N-B6N.

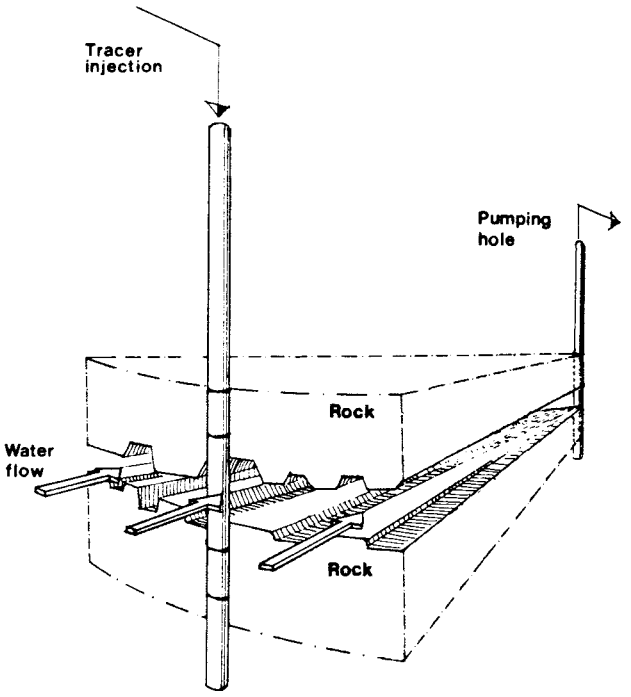

Figure 3-1 Fracture with different apertures.

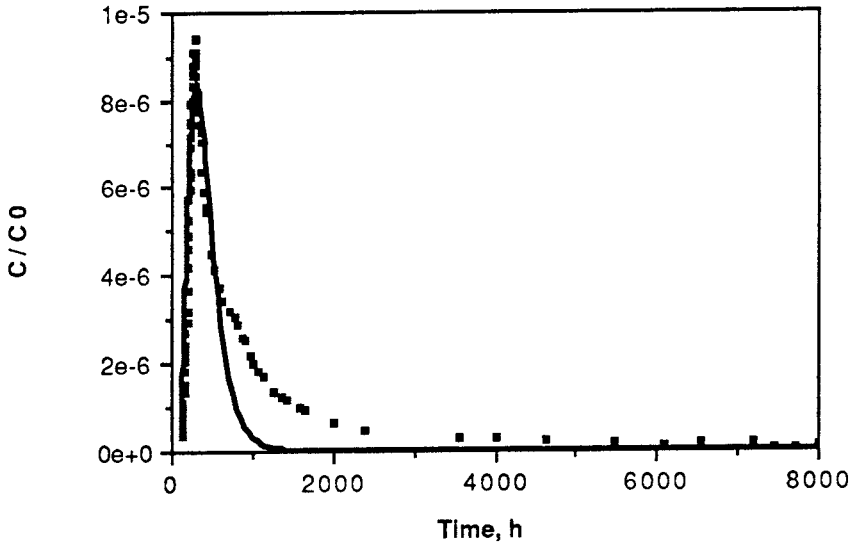

Figure 5-1 Curve fitted using the AD model with one pathway. Run B1N-B6N for the nonsorbing tracer tritiated water.

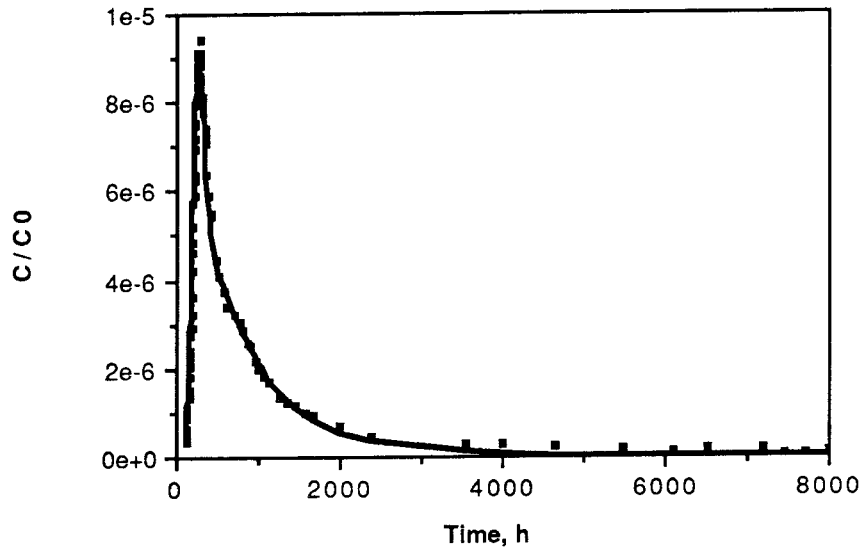

Figure 5-2 Curve fitted using the AD model with two pathways. Run B1N-B6N for the nonsorbing tracer tritiated water. The dispersivity and residence time are different in the two different channels.

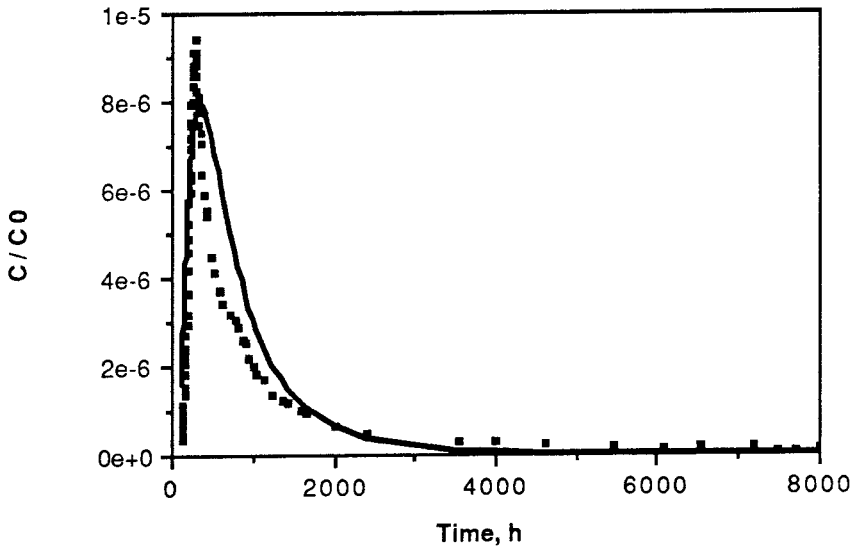

Figure 5-3 Curve fitted using the AD model with one pathway with total proportionality factor determined from the experimental data. Run B1N-B6N for the nonsorbing tracer tritiated water.

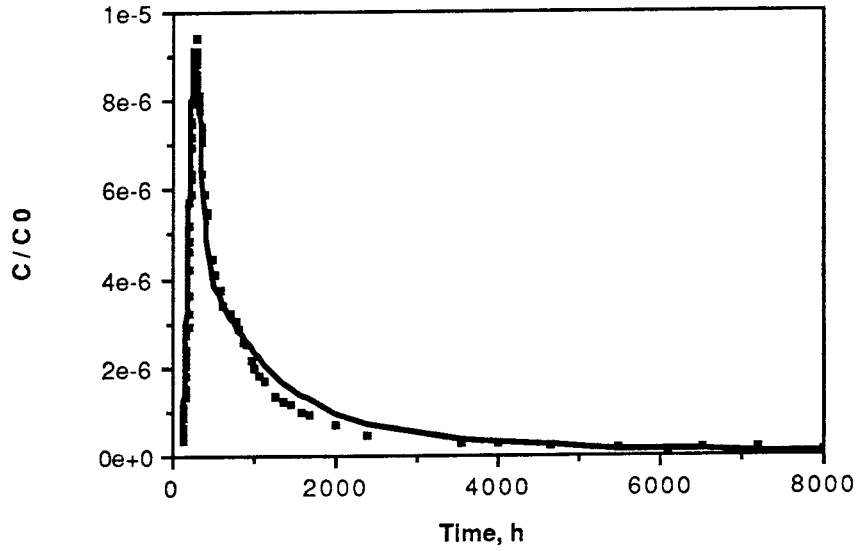

Figure 5-4 Curve fitted using the AD model with two pathways with total proportionality factor determined from the experimental data. Run B1N-B6N for the nonsorbing tracer tritiated water.

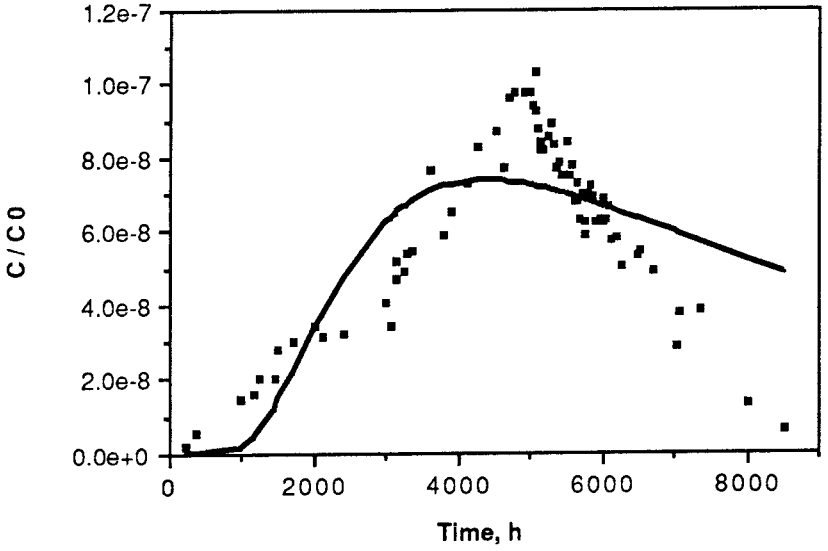

Figure 5-5 Curve fitted using the AD model with one pathway with Peclet number and proportionality factor from nonsorbing tracer test. Fit includes tracer residence time and loss factor. Run B1N-B6N for the sorbing tracer strontium.

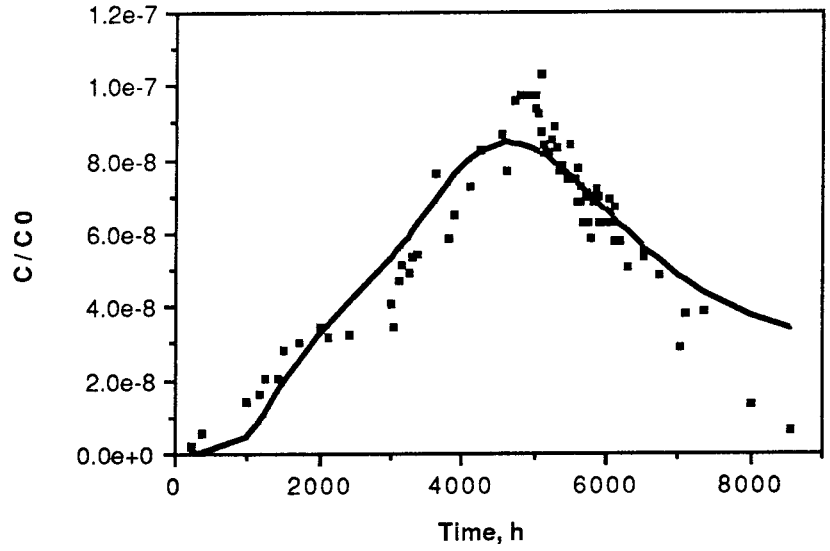

Figure 5-6 Curve fitted using the AD model with two pathways with Peclet number and proportionality factor from nonsorbing tracer test. Fit includes tracer residence time and loss factor. Run B1N-B6N for the sorbing tracer strontium.

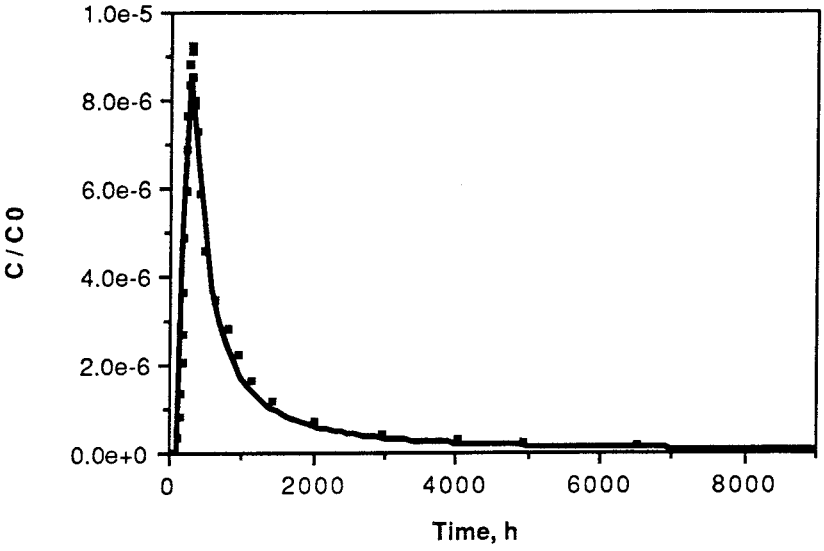

Figure 6-1 Curve fitted using the ADD model with the proportionality factor determined from experimental data. Run B1N-B6N for the nonsorbing tracer tritiated water.

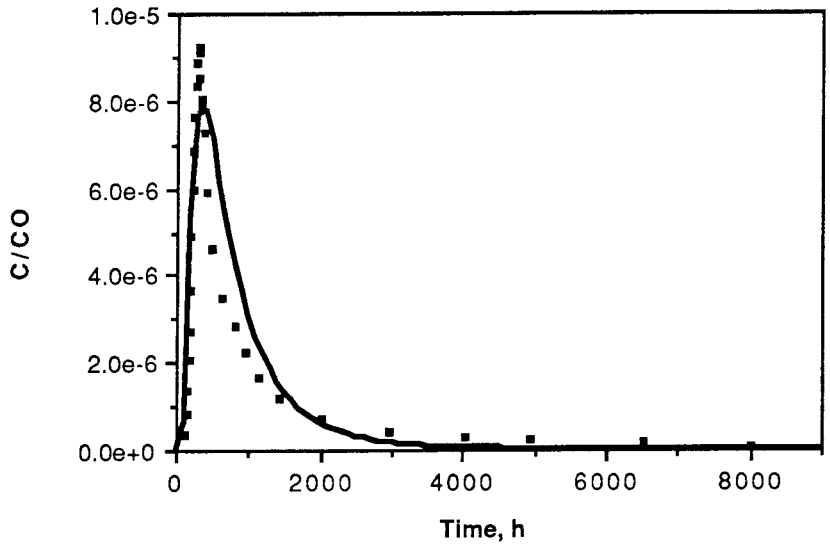

Figure 6-2 Curve fitted using the ADD model with the A-parameter determined using $D_e \cdot \varepsilon_p = 0.006 \cdot 10^{-12}$ m^2/s and the proportionality factor determined from experimental data. Run B1N-B6N for the nonsorbing tracer tritiated water.

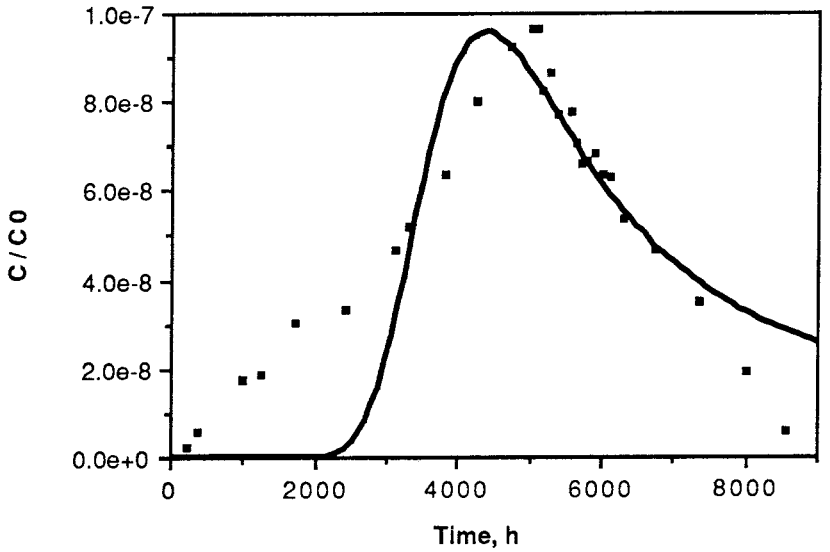

Figure 6-3 Curve fitted using the ADD model with Peclet number from nonsorbing tracer test (Table 6-1, column 1). Run B1N-B6N for the sorbing tracer strontium.

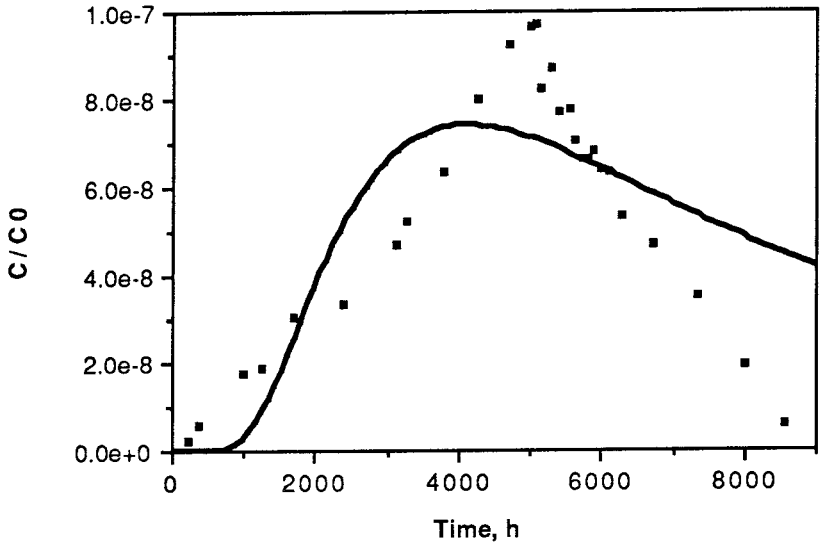

Figure 6-4 Curve fitted using the ADD model with Peclet number from nonsorbing tracer test (Table 6-1, column 2). Run B1N-B6N for the sorbing tracer strontium.

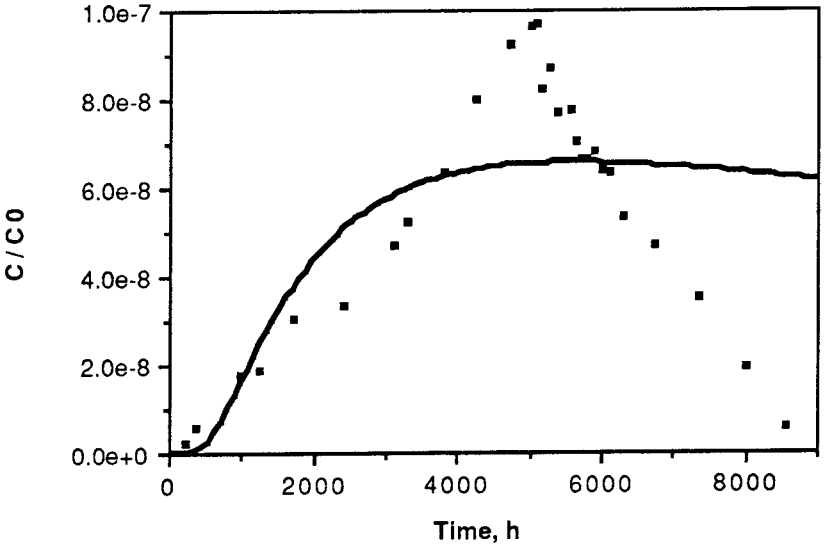

Figure 6-5 Curve fitted using the ADD model with Peclet number and proportionality factor from nonsorbing tracer test (Table 6-1, column 2). Run B1N-B6N for the sorbing tracer strontium.

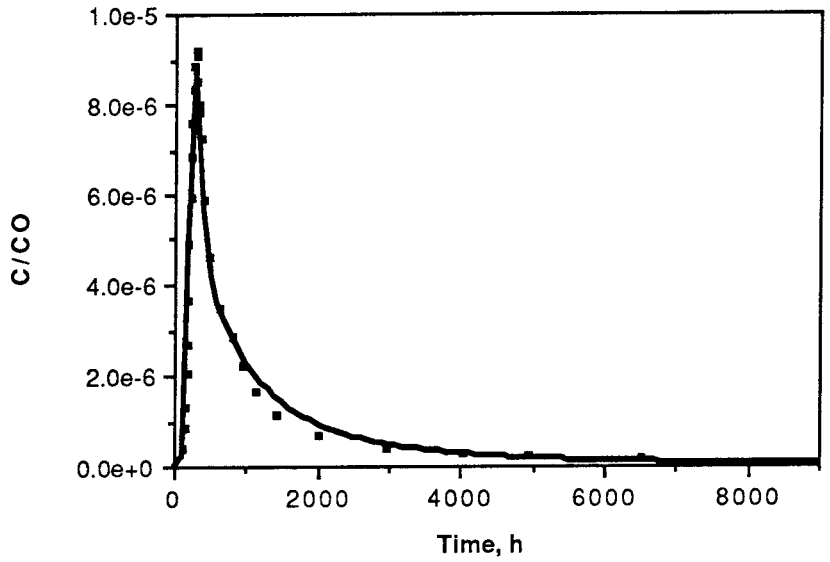

Figure 6-6 Curve fitted using the ADD model with two pathways with the A-parameter determined using $D_e \cdot \varepsilon_p = 0.006 \cdot 10^{-12}$ m^2/s and the total proportionality factor determined from experimental data. Run B1N-B6N for the nonsorbing tracer tritiated water.

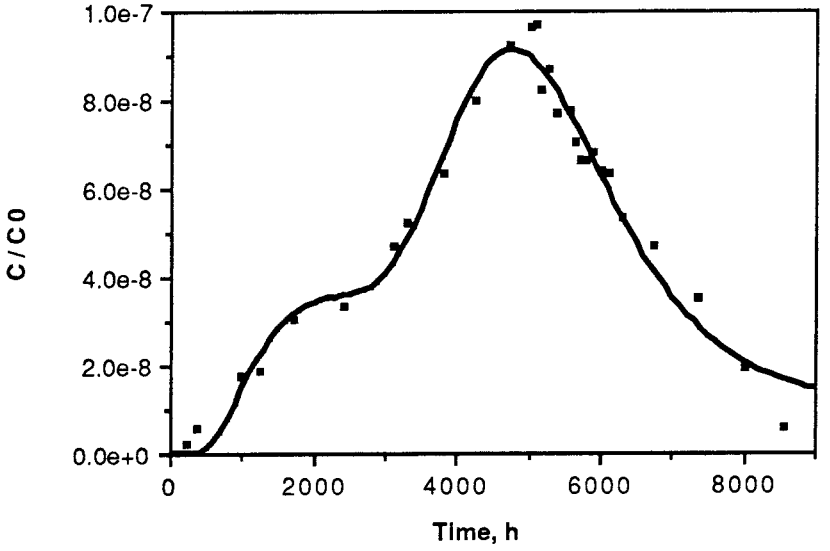

Figure 6-7 Curve fitted using the ADD model with two pathways with Peclet numbers from nonsorbing tracer test. Run B1N-B6N for the sorbing tracer strontium.

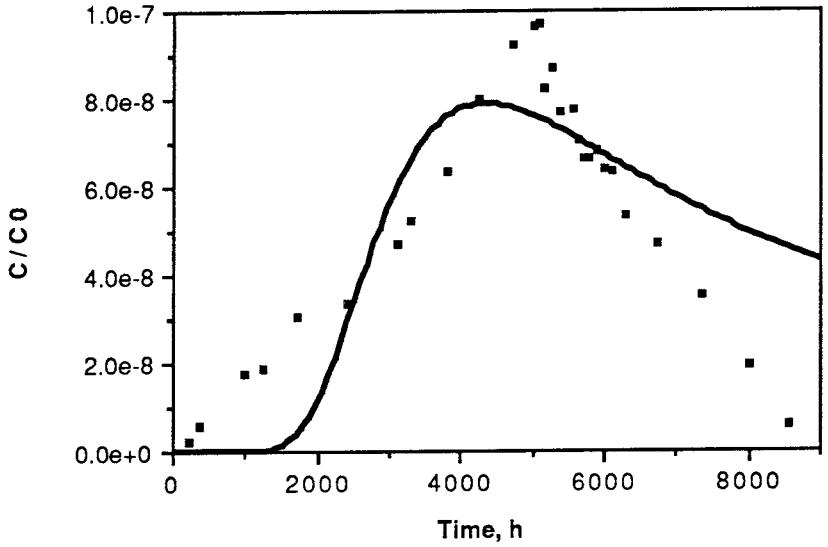

Figure 6-8 Curve fitted using the ADD model with two pathways with Peclet numbers and proportionality factors from nonsorbing tracer test. Run B1N-B6N for the sorbing tracer strontium.

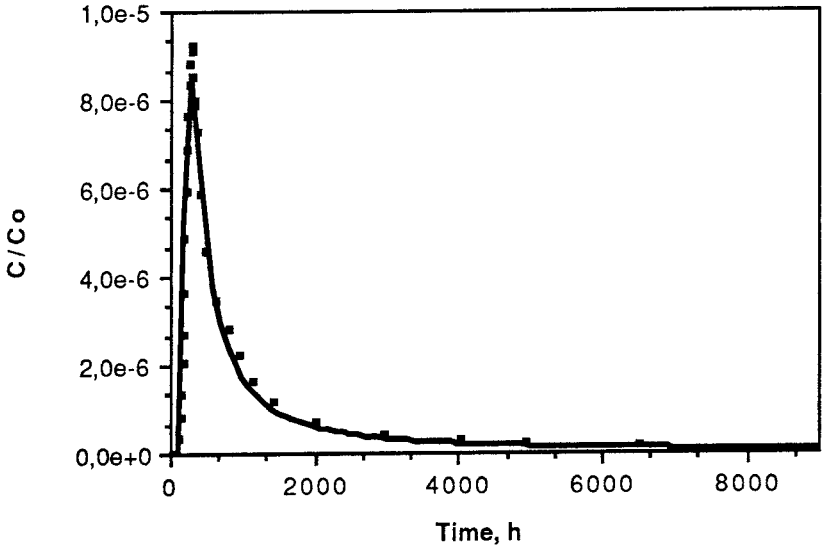

Figure 7-1 Curve fitted using the ACD model with the proportionality factor determined from experimental data. Run B1N-B6N for the nonsorbing tracer tritiated water.

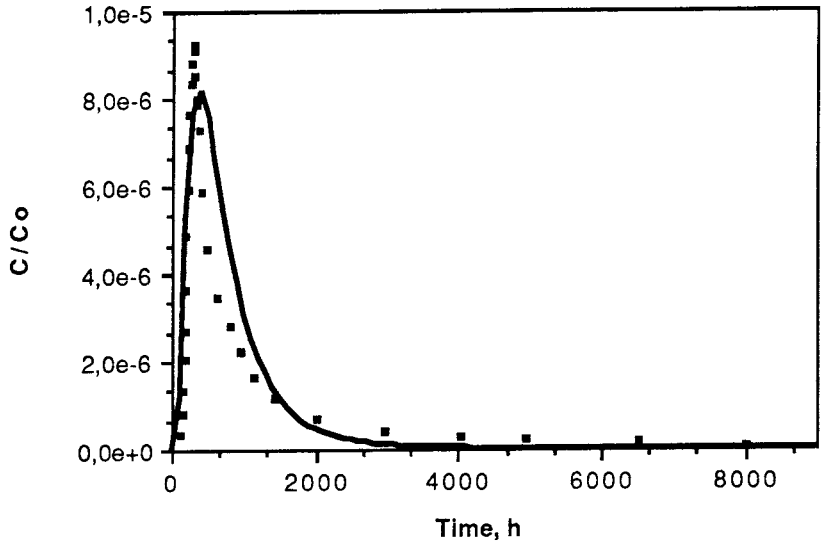

Figure 7-2 Curve fitted using the ACD model with the B-parameter determined using $D_e \cdot \varepsilon_p = 0.006 \cdot 10^{-12}$ m^2/s and the proportionality factor determined from experimental data. Run B1N-B6N for the nonsorbing tracer tritiated water.

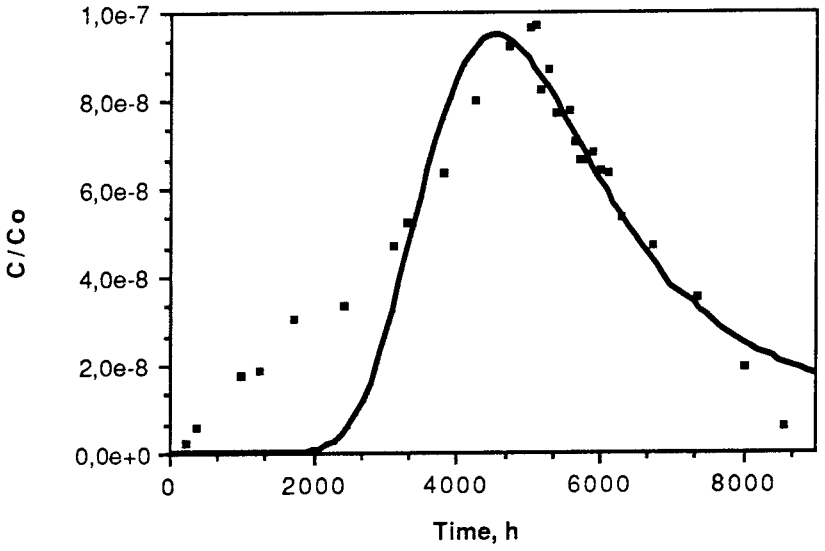

Figure 7-3 Curve fitted using the ACD model with the standard deviation in the lognormal distribution from the nonsorbing tracer test (Table 7-1, column 1). Run B1N-B6N for the sorbing tracer strontium.

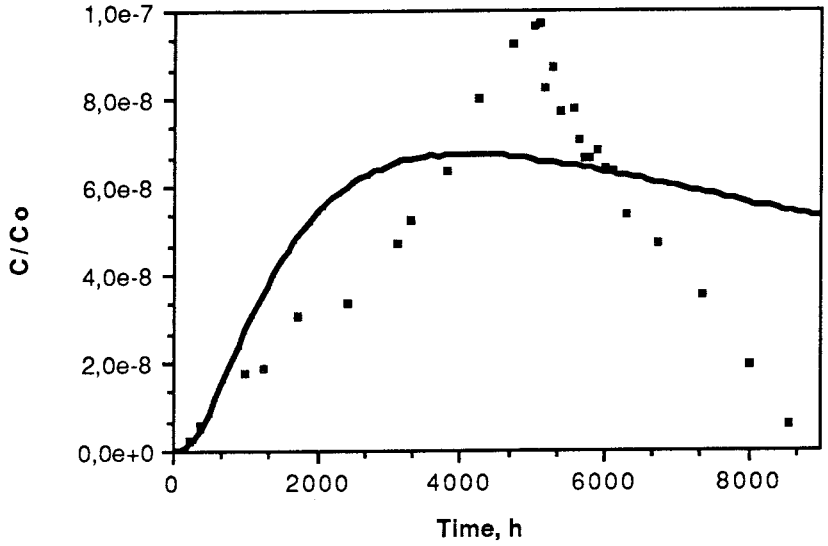

Figure 7-4 Curve fitted using the ACD model with the standard deviation in the lognormal distribution from nonsorbing tracer test (Table 7-1, column 2). Run B1N-B6N for the sorbing tracer strontium.

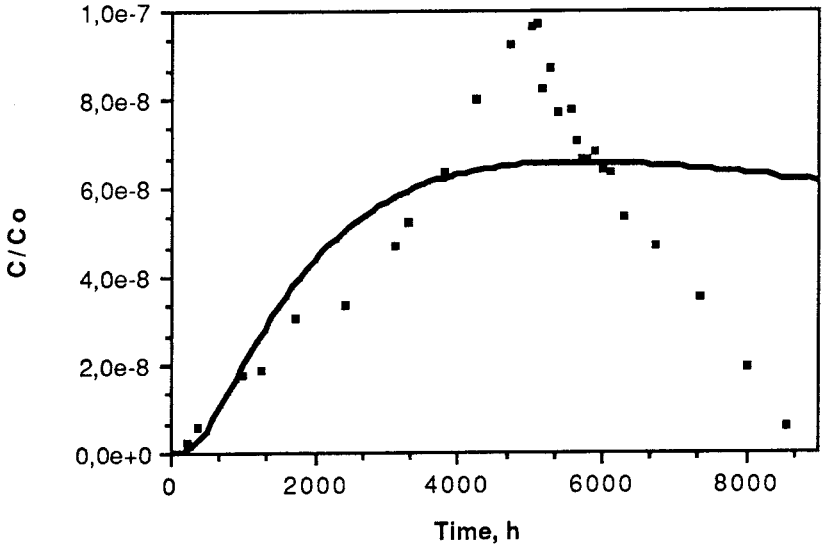

Figure 7-5 Curve fitted using the ACD model with the standard deviation in the lognormal distribution and proportionality factor from nonsorbing tracer test (Table 7-1, column 2). Run B1N-B6N for the sorbing tracer strontium.

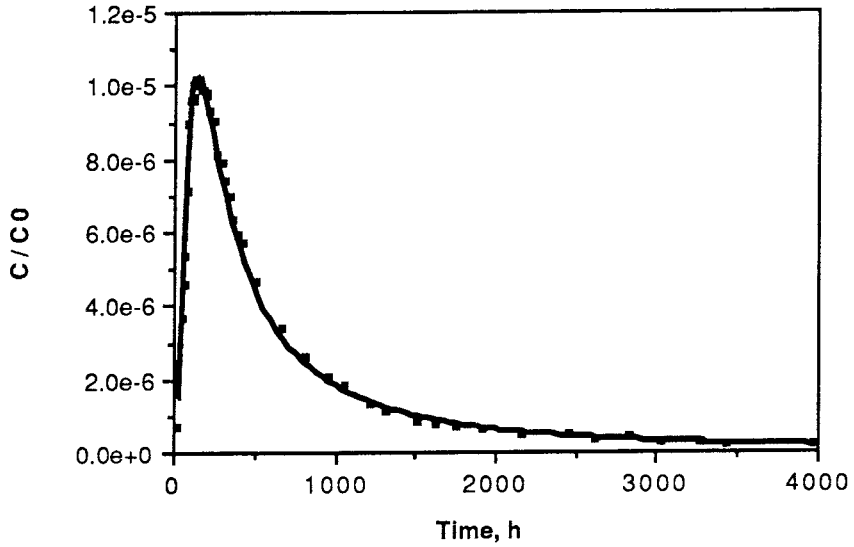

Figure 8-1 Curve fitted using the AD model with one pathway with total proportionality factor determined from the experimental data. Run B5N-B6N for the nonsorbing tracer tritiated water.

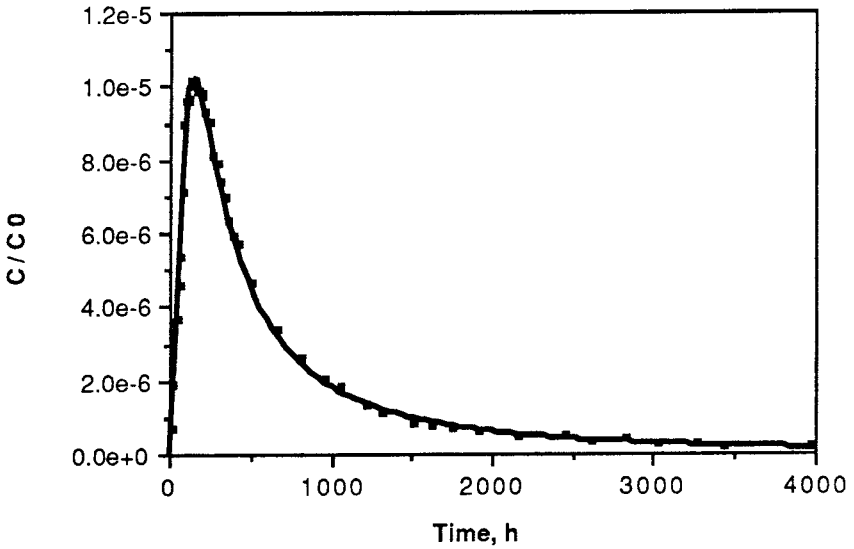

Figure 8-2 Curve fitted using the AD model with two pathways with total proportionality factor determined from the experimental data. Run B5N-B6N for the nonsorbing tracer tritiated water.

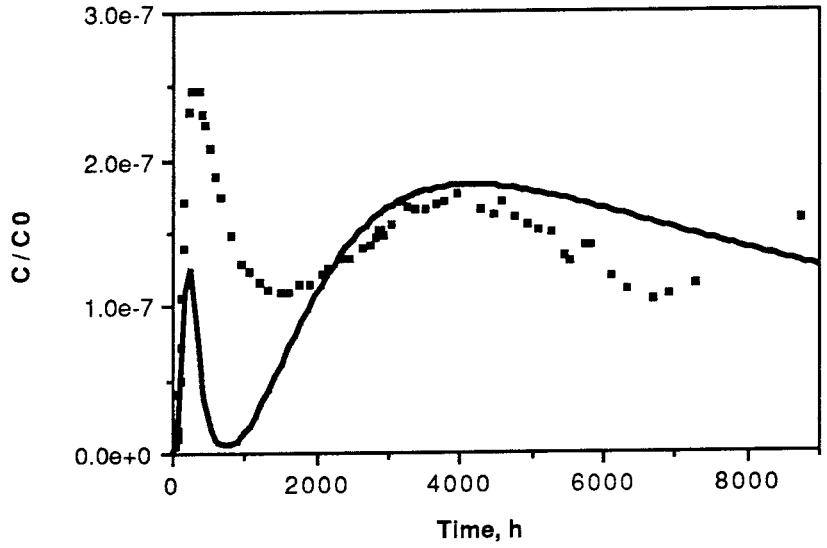

Figure 8-3 Curve fitted using the AD model with two pathways with Peclet numbers and proportionality factors from nonsorbing tracer test. Fit includes tracer residence times and loss factor. Run B5N-B6N for the sorbing tracer strontium.

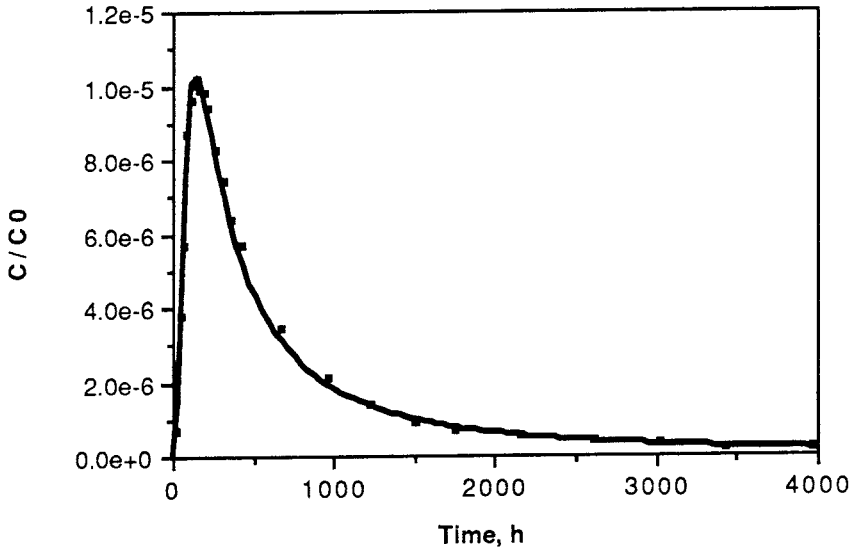

Figure 8-4 Curve fitted using the ADD model with the proportionality factor determined from experimental data. Run B5N-B6N for the nonsorbing tracer tritiated water.

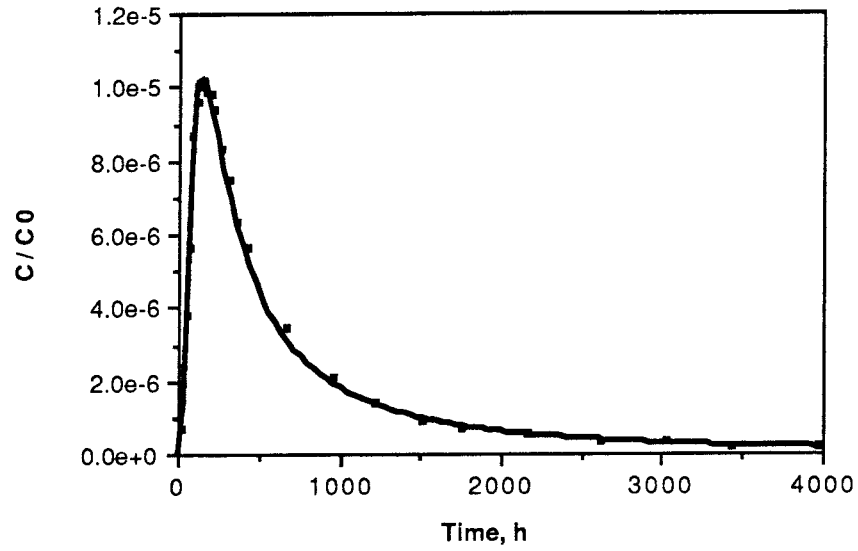

Figure 8-5 Curve fitted using the ADD model with the A-parameter determined using $D_e \cdot \varepsilon_p = 0.006 \cdot 10^{-12}$ m^2/s and the proportionality factor determined from experimental data. Run B5N-B6N for the nonsorbing tracer tritiated water.

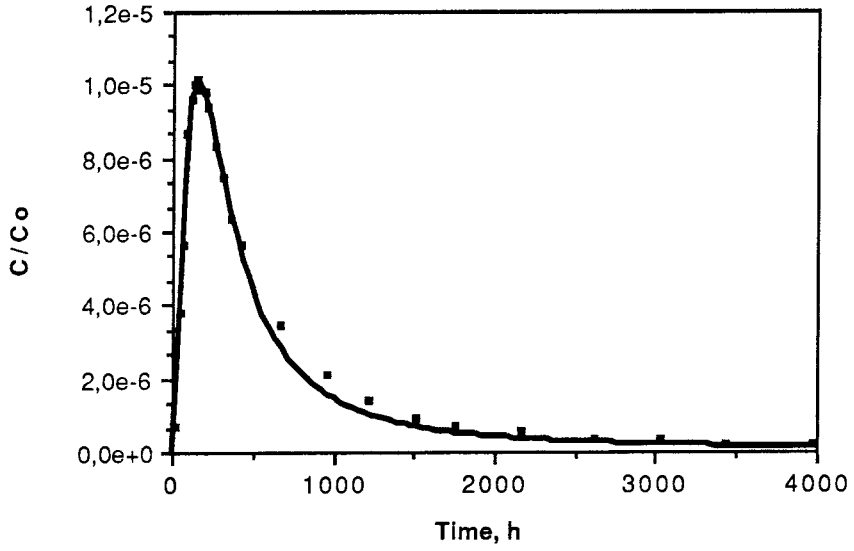

Figure 8-6 Curve fitted using the ACD model with the proportionality factor determined from experimental data. Run B5N-B6N for the nonsorbing tracer tritiated water.

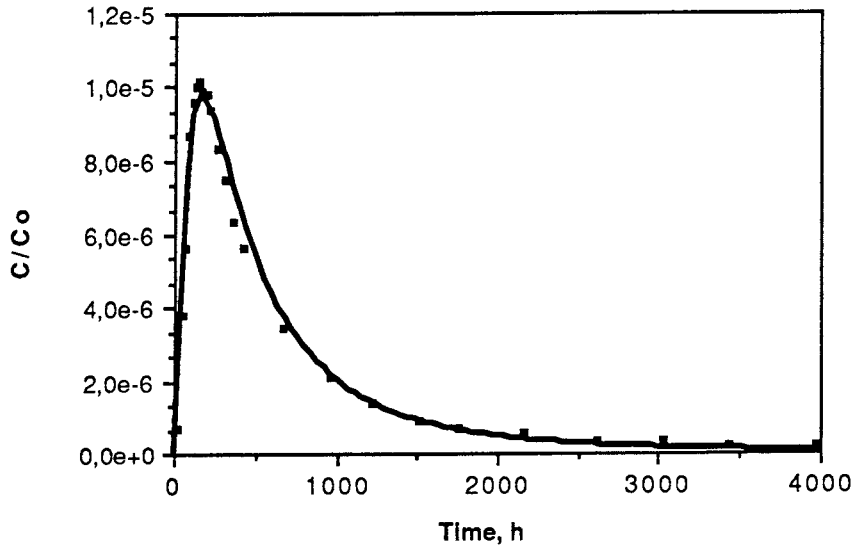

Figure 8-7 Curve fitted using the ACD model with the B-parameter determined using $D_e \cdot \varepsilon_p = 0.006 \cdot 10^{-12}$ m^2/s and the proportionality factor determined from experimental data. Run B5N-B6N for the nonsorbing tracer tritiated water.

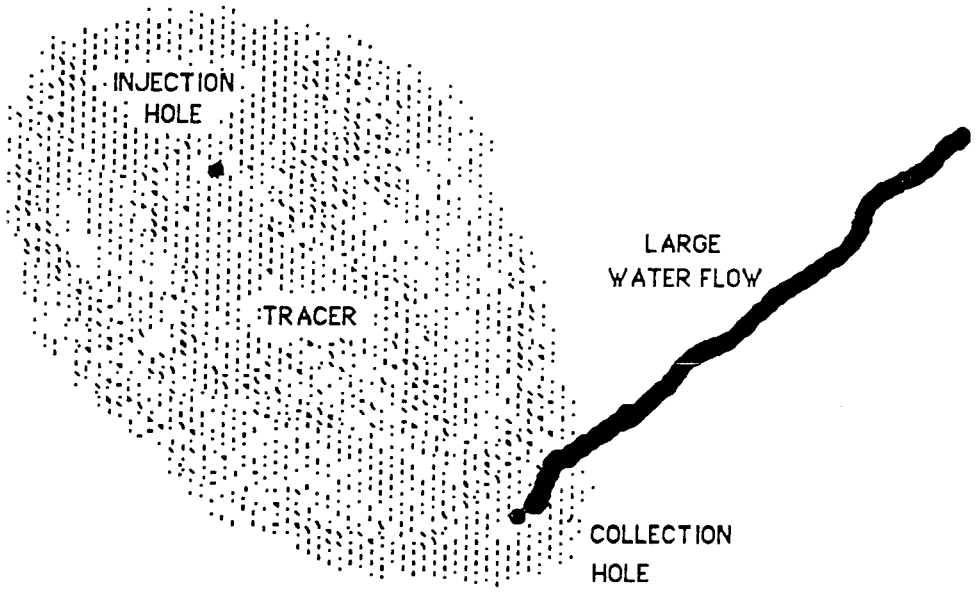

Figure 9-1 Possible flow situation into one channel system.

APPENDIX A.

Run B1N-B6N-TRITIATED WATER

time hrs	C/Co $\cdot 10^6$	time hrs	C/Co $\cdot 10^6$	time hrs	C/Co $\cdot 10^6$
121	0.380	257	8.63	688	3.82
125	0.515	261	8.84	706	3.59
130	0.667	265	9.09	715	3.43
135	0.850	269	8.45	756	3.55
140	1.00	273	9.12	768	3.05
145	1.09	277	9.12	814	2.87
150	1.37	281	9.03	862	2.56
155	1.51	285	9.05	910	2.52
160	1.82	289	9.42	958	2.18
165	2.06	293	8.99	1005	2.00
169	2.25	297	8.81	1053	1.82
173	2.42	301	8.57	1145	1.72
177	2.73	305	8.21	1250	1.34
181	2.92	309	8.14	1358	1.24
185	3.19	313	7.93	1436	1.15
189	3.65	317	8.10	1584	1.02
193	4.19	321	7.82	1668	0.926
197	4.61	325	7.90	2010	0.673
201	4.87	329	7.79	2400	0.482
205	5.22	339	7.45	3118	0.023
209	5.72	349	7.28	3552	0.312
213	5.93	359	7.05	4008	0.306
217	6.26	370	6.38	4632	0.227
221	6.38	391	5.91	5472	0.187
225	6.95	409	5.51	6096	0.120
229	7.19	430	5.44	6530	0.151
233	7.49	481	4.46	7200	0.203
237	7.52	529	4.10	7464	0.070
241	7.94	571	3.73	7704	0.076
245	8.01	619	3.41	8016	0.099
249	8.35	655	1.02	8544	0.074
253	8.60	670	2.08	9240	0.041

Run B1N-B6N-STRONTIUM

time hrs	C/Co $\cdot 10^7$	time hrs	C/Co $\cdot 10^7$	time hrs	C/Co $\cdot 10^7$
217	0.209	4248	0.827	5718	0.699
266	0.384	4524	0.870	5740	0.627
314	0.344	4620	0.771	5772	0.589
366	0.258	4710	0.962	5796	0.702
510	0.203	4785	0.976	5830	0.685
738	0.180	4902	0.976	5844	0.721
984	0.184	4994	0.976	5876	0.696
988	0.204	5026	0.941	5904	0.625
1154	0.162	5054	0.926	5976	0.631
1243	0.202	5074	1.03	5996	0.627
1440	0.207	5102	0.877	6030	0.691
1510	0.282	5126	0.842	6066	0.629
1704	0.304	5153	0.820	6096	0.669
2016	0.347	5189	0.820	6118	0.576
2112	0.319	5231	0.856	6190	0.581
2400	0.325	5273	0.891	6278	0.506
2998	0.406	5308	0.835	6502	0.533
3048	0.347	5340	0.771	6530	0.549
3118	0.470	5388	0.785	6720	0.488
3144	0.516	5444	0.750	7032	0.286
3238	0.491	5500	0.842	7080	0.382
3276	0.538	5548	0.750	7200	0.644
3361	0.544	5586	0.778	7344	0.389
3612	0.764	5596	0.682	8016	0.132
3800	0.587	5638	0.728	8544	<0.060
3894	0.652	5652	0.682	8736	<0.071
4104	0.728	5684	0.629		

RunB5N-B6N-TRITIATED WATER.

time hrs	C/Co $\cdot 10^6$	time hrs	C/Co $\cdot 10^6$	time hrs	C/Co $\cdot 10^6$
16	0.69	189	9.76	1053	1.84
24	1.92	199	9.85	1224	1.38
49	3.68	215	9.33	1321	1.15
57	4.56	237	9.00	1510	0.878
69	5.37	261	8.14	1623	0.808
79	7.14	285	7.92	1753	0.726
89	8.96	309	7.44	1918	0.628
99	9.61	335	6.97	2160	0.508
109	9.61	363	6.35	2448	0.501
119	9.65	387	5.91	2616	0.324
129	10.14	417	5.73	2826	0.390
139	10.17	498	4.69	3024	0.307
149	10.01	670	3.38	3264	0.265
159	9.99	816	2.60	3432	0.227
169	9.89	960	2.04	3690	0.184
179	9.89				

Run B5N-B6N-STRONTIUM.

time hrs	C/Co $\cdot 10^7$	time hrs	C/Co $\cdot 10^7$	time hrs	C/Co $\cdot 10^7$
19	-	1224	1.16	3768	1.72
49	0.05	1321	1.11	3936	1.77
65	0.11	1510	1.10	4296	1.66
69	0.155	1623	1.09	4464	1.63
73	0.155	1753	1.14	4584	1.71
88	0.401	1918	1.15	4680	0.288
93	0.489	2089	1.22	4800	1.10
103	0.727	2160	1.26	4896	0.126
120	1.06	2354	1.33	5016	0.70
140	1.40	2448	1.33	5112	0.893
154	1.71	2616	1.39	5184	1.03
224	2.33	2759	1.42	5304	1.21
258	2.47	2826	1.47	5448	1.35
350	2.47	2854	1.52	5520	1.30
402	2.32	2879	1.52	5736	1.42
450	2.25	2929	1.48	5808	1.41
498	2.09	3024	1.55	6120	1.40
570	1.89	3166	1.72	6333	0.913
670	1.75	3264	1.67	6700	1.05
816	1.49	3360	1.65	6911	1.07
960	1.29	3528	1.66	7287	1.14
1053	1.23	3648	1.69	8727	1.59

APPENDIX B.

Table B-1. Packer location in the injection holes and length of the flow paths.

Injection hole	Packers injection	Location withdrawal	Distance
B1N	91.0-92.3 m	94-102 m	11.8 m
B5N	78.8-80.1 m	66- 66 m	14.6 m

Table B-2. Data on the Sr-85 and Cs-134 migration tests.

Flow path	Tracer injected	Chemical form	Total radio-activity	Concentration (carriers included)
B1N-B6N	I-131	NaI	352 MBq	$8.0\ 10^{-2}$ M
	H-3	Tritiated water	357 MBq	
	Sr-85	$SrCl_2$	707 MBq	$1.0\ 10^{-4}$ M
B5N-B6N	I-131	NaI	309 MBq	
	H-3	Tritiated water	345 MBq	
	Sr-85	$SrCl_2$	750 MBq	$1.1\ 10^{-4}$ M
	Cs-134	CsCl	1280 MBq	$4.0\ 10^{-5}$ M

List of SKB reports

Annual Reports

1977–78
TR 121
KBS Technical Reports 1 – 120.
Summaries. Stockholm, May 1979.

1979
TR 79–28
The KBS Annual Report 1979.
KBS Technical Reports 79-01 – 79-27.
Summaries. Stockholm, March 1980.

1980
TR 80–26
The KBS Annual Report 1980.
KBS Technical Reports 80-01 – 80-25.
Summaries. Stockholm, March 1981.

1981
TR 81–17
The KBS Annual Report 1981.
KBS Technical Reports 81-01 – 81-16.
Summaries. Stockholm, April 1982.

1982
TR 82–28
The KBS Annual Report 1982.
KBS Technical Reports 82-01 – 82-27.
Summaries. Stockholm, July 1983.

1983
TR 83–77
The KBS Annual Report 1983.
KBS Technical Reports 83-01 – 83-76
Summaries. Stockholm, June 1984.

1984
TR 85–01
Annual Research and Development Report 1984
Including Summaries of Technical Reports Issued during 1984. (Technical Reports 84-01– 84-19)
Stockholm June 1985.

1985
TR 85-20
Annual Research and Development Report 1985
Including Summaries of Technical Reports Issued during 1985. (Technical Reports 85-01-85-19)
Stockholm May 1986.

1986
TR 86-31
SKB Annual Report 1986
Including Summaries of Technical Reports Issued during 1986
Stockholm, May 1987

1987
TR 87-33
SKB Annual Report 1987
Including Summaries of Technical Reports Issued during 1987
Stockholm, May 1988

1988
TR 88-32
SKB Annual Report 1988
Including Summaries of Technical Reports Issued during 1988
Stockholm, May 1989

Technical Reports

1989
TR 89-01
Near-distance seismological monitoring of the Lansjärv neotectonic fault region Part II: 1988
Rutger Wahlström, Sven-Olof Linder,
Conny Holmqvist, Hans-Edy Mårtensson
Seismological Department, Uppsala University,
Uppsala
January 1989

TR 89-02
Description of background data in SKB database GEOTAB
Ebbe Eriksson, Stefan Sehlstedt
SGAB, Luleå
February 1989

TR 89-03
Characterization of the morphology, basement rock and tectonics in Sweden
Kennert Röshoff
August 1988

TR 89-04
SKB WP-Cave Project
Radionuclide release from the near-field in a WP-Cave repository
Maria Lindgren, Kristina Skagius
Kemakta Consultants Co, Stockholm
April 1989

TR 89-05
SKB WP-Cave Project
Transport of escaping radionuclides from the WP-Cave repository to the biosphere
Luis Moreno, Sue Arve, Ivars Neretnieks
Royal Institute of Technology, Stockholm
April 1989

TR 89-06
SKB WP-Cave Project
Individual radiation doses from nuclides contained in a WP-Cave repository for spend fuel
Sture Nordlinder, Ulla Bergström
Studsvik Nuclear, Studsvik
April 1989

TR 89-07
SKB WP-Cave Project
Some Notes on Technical Issues

TR 89-08
SKB WP-Cave Project
Thermally incuded convective motion in groundwater in the near field of the WP-Cave after filling and closure
Polydynamics Limited, Zürich
April 1989